

**UNIVERSIDADE FEDERAL DO RIO GRANDE DO SUL  
INSTITUTO DE GEOCIÊNCIAS  
PROGRAMA DE PÓS-GRADUAÇÃO EM GEOCIÊNCIAS**

**INSIGHTS GEOQUÍMICOS SOBRE AS INFLUÊNCIAS  
PALEOAMBIENTAIS NA DEPOSIÇÃO DE FOLHELHOS  
RICOS EM MATÉRIA ORGÂNICA NO MAR IRATI-  
WHITEHILL, SUL DA BACIA DO PARANÁ**

**JHENIFER CAROLINE DA SILVA PAIM**

**ORIENTADORA – Prof<sup>a</sup> Dra. Juliana Charão Marques**

**COORIENTADOR – Prof<sup>a</sup> Dra. Karin Goldberg**

**Porto Alegre, 2024**

**UNIVERSIDADE FEDERAL DO RIO GRANDE DO SUL  
INSTITUTO DE GEOCIÊNCIAS  
PROGRAMA DE PÓS-GRADUAÇÃO EM GEOCIÊNCIAS**

**INSIGHTS GEOQUÍMICOS SOBRE AS INFLUÊNCIAS  
PALEOAMBIENTAIS NA DEPOSIÇÃO DE FOLHELHOS  
RICOS EM MATÉRIA ORGÂNICA NO MAR IRATI-  
WHITEHILL, SUL DA BACIA DO PARANÁ**

**JHENIFER CAROLINE DA SILVA PAIM**

ORIENTADORA – Prof<sup>a</sup> Dra. Juliana Charão Marques

COORIENTADOR – Prof<sup>a</sup> Dra. Karin Goldberg

**BANCA EXAMINADORA**

Prof. Dr. Ailton da Silva Brito – Universidade Federal Do Vale Do São Francisco

Prof<sup>a</sup>. Dr<sup>a</sup>. Rosalia Barili Da Cunha– Instituto Do Petróleo e dos Recursos Naturais,  
Pontifícia Universidade Católica Do Rio Grande Do Sul

Prof<sup>a</sup>. Dra. Taís Freitas da Silva– Instituto De Geociências, Universidade Federal Do  
Rio Grande Do Sul

Dissertação de Mestrado apresentada  
como requisito parcial para a obtenção do  
Título De Mestre Em Ciências.

Porto Alegre, 2024

### CIP - Catalogação na Publicação

Paim, Jhenifer Caroline da Silva  
INSIGHTS GEOQUÍMICOS SOBRE AS INFLUÊNCIAS  
PALEOAMBIENTAIS NA DEPOSIÇÃO DE FOLHELHOS RICOS EM  
MATÉRIA ORGÂNICA NO MAR IRATI-WHITEHILL, SUL DA BACIA  
DO PARANÁ / Jhenifer Caroline da Silva Paim. --  
2024.

65 f.

Orientadora: Juliana Charão Marques.

Coorientadora: Karin Goldberg.

Dissertação (Mestrado) -- Universidade Federal do  
Rio Grande do Sul, Instituto de Geociências, Programa  
de Pós-Graduação em Geociências, Porto Alegre, BR-RS,  
2024.

1. Folhelhos ricos em matéria orgânica. 2. anoxia .  
3. paleoambiente. 4. proxies geoquímicos. 5.  
químioestratigrafia. I. Marques, Juliana Charão,  
orient. II. Goldberg, Karin, coorient. III. Título.

## AGRADECIMENTOS

A realização deste trabalho só foi possível graças ao apoio e à dedicação de várias pessoas, às quais sou profundamente grata.

Agradeço, em primeiro lugar, à minha família, que nunca poupou esforços para me ajudar a conquistar meus sonhos. Sempre me apoiou e deu forças nos momentos mais desafiadores, compreendendo os momentos delicados da jornada.

Ao meu namorado e parceiro, Guilherme, por sua enorme paciência e incentivo ininterrupto. Por ser sempre esse companheiro preocupado e atencioso, me lembrando de respirar, rir e aproveitar. Muito obrigada; você foi fundamental para que eu pudesse alcançar este objetivo.

Aos meus amigos Paula e Vitor, que, nos aguardadíssimos momentos de pausa, me lembravam dos meus verdadeiros motivos. Aos copos cheios e às amizades duradouras, que minha vitória seja a de vocês também. Sem nossas risadas, o caminho certamente teria sido mais difícil.

Aos colegas de bolsa, muito obrigada pelos cafezinhos e pelos momentos de foco indispensáveis. Em especial a Daniela, Marina e Adriana: gurias, a gente consegue, sigam em frente!

Agradeço imensamente à Juliana e à Karin pela orientação e pelas palavras de encorajamento, que me ajudaram a superar os obstáculos ao longo do caminho.

Por fim, agradeço à PETROBRAS (00500071791119), cujo apoio financeiro e parceria foram essenciais para a execução deste trabalho. E também ao Programa de Recursos Humanos da Agência Nacional do Petróleo, Gás Natural e Biocombustíveis (PRH-ANP), com recursos fornecidos pelas empresas de petróleo sob a cláusula contratual nº 50/2015 de P&D&I da ANP.

## RESUMO

O Mar Irati-Whitehill era um vasto mar epicontinental no paleocontinente Gondwana durante o Permiano Inferior. A Formação Irati representa este antigo mar na Bacia do Paraná, Brasil. Na parte sul da bacia, são identificados dois intervalos de folhelhos ricos em matéria orgânica, sendo o inferior com os maiores níveis de carbono orgânico total (COT). Para elucidar as condições que desencadearam o acúmulo de matéria orgânica (MO) no folhelho inferior, este estudo integra descrições de fácies e petrográficas com dados geoquímicos e isotópicos de dois poços na parte sul da Bacia do Paraná. Os intervalos foram subdivididos pela evolução paleoambiental da anóxia em um ambiente lacustre ou marinho restrito que permitiu a deposição de folhelhos ricos em matéria orgânica. O intervalo estudado inicia com uma deposição em um ambiente salino e com baixa concentração de matéria orgânica (intervalo pré-orgânico), que gradativamente apresenta redução na salinidade, aumento na produtividade primária e crescimento da anóxia, culminando em um aumento no conteúdo orgânico (intervalo de incremento orgânico). A máxima concentração de matéria orgânica (15% TOC) ocorre associada a baixa salinidade e alta produtividade primária, e é bem marcada por condições anóxicas a euxínicas (intervalo de estabilidade orgânica). Isso sugere um ambiente que experimentou um influxo de água doce que desencadeou um crescimento microbiano que levou ao esgotamento de oxigênio e preservação de MO. Após essa alta acumulação de MO, o ambiente torna-se oxigenado, com aporte detrítico regular e sem alta produtividade primária no intervalo de baixa matéria orgânica. Condições semelhantes foram observadas em outras bacias ao redor do mundo, como a Bacia de Cariaco, que é uma bacia restrita com ressurgências episódicas, considerada como uma variação redox de baixa frequência. A Bacia Irati-Whitehill espelha a dinâmica observada na Bacia de Cariaco, sendo uma bacia restrita com aporte episódico de água doce.

**PALAVRAS-CHAVE:** Folhelhos ricos em matéria orgânica, paleoambiental, quimioestratigrafia, anóxia, produtividade primária, salinidade

## ABSTRACT

The Irati-Whitehill Sea was a vast epicontinental sea on the paleocontinent Gondwana during the Lower Permian. In Brazil's Paraná Basin, the Irati Formation represents this ancient sea. In the southern part of the basin, two intervals of organic-rich shales are identified, with the lowermost one displaying the highest levels of total organic carbon (TOC). To elucidate the conditions that triggered organic matter (OM) accumulation in the lower shale, this study integrates facies and petrographic descriptions with geochemical and isotopic data from two wells in the southern Paraná Basin. The intervals were subdivided based on the paleoenvironmental evolution of anoxia in a lacustrine or restricted marine environment, which allowed the deposition of organic-rich shales. The studied interval begins with deposition in a saline environment with low organic matter concentration (pre-organic interval), where salinity gradually decreases, primary productivity increases, and anoxia intensifies, culminating in an increase in organic content (organic increment interval). The highest concentration of organic matter (15% TOC) occurs alongside low salinity and high primary productivity, and is well-marked by anoxic to euxinic conditions (organic stability interval). This suggests an environment where freshwater influx triggered a microbial bloom, leading to oxygen depletion and OM preservation. After this peak in OM accumulation, the environment became oxygenated, with regular detrital input and low primary productivity in the low-organic interval. Similar conditions have been observed in other basins worldwide, such as the Cariaco Basin, a restricted basin with episodic upwellings considered as a low-frequency temporal redox system. Therefore, the Irati-Whitehill Basin parallels the dynamics observed in the Cariaco Basin, functioning as a restricted basin with episodic freshwater input.

**KEYWORDS:** Organic-rich shales, paleoenvironmental, chemostratigraphy, anoxic, primary productivity, salinity

## SUMÁRIO

<b>CAPITULO I TEXTO INTEGRADOR</b> .....	7
1. INTRODUÇÃO .....	7
1.1 OBJETIVOS.....	8
2. ANOXIA EM BACIAS.....	8
2.1 TERMINOLOGIA DA CONCENTRAÇÃO DE OXIGÊNIO NO SISTEMA .....	8
3. PROXIES GEOQUÍMICOS PARA ESTUDOS PALEOAMBIENTAIS .....	11
4 BACIA DO PARANÁ.....	15
4.1 FORMAÇÃO IRATI.....	18
5 MATERIAIS E MÉTODOS .....	20
<b>CAPITULO II ARTIGO</b> .....	23
ANEXO A – COMPROVANTES DE SUBMISSÃO DO ARTIGO.....	64

## CAPITULO I TEXTO INTEGRADOR

### 1. INTRODUÇÃO

Estudos realizados em diversas bacias ao redor do mundo utilizam a quimioestratigrafia para entender os fatores propiciam condições para a deposição e preservação de matéria orgânica (MO) (Berner & Raiswell, 1984; Jones & Manning, 1994; Murphy et al., 2000; McArthur, J. et al., 2008; Algeo, T.J. & Tribovillard, 2009; Sweere et al., 2016; McArthur, J. M., 2019). A preservação e a acumulação dessa MO são influenciadas por vários fatores paleodeposicionais, sendo os principais a produtividade primária e as condições oxi-redutoras do ambiente. Rochas finas, como os folhelhos ricos em matéria orgânica, fazem parte de um contexto evolutivo mais amplo da bacia. Sua deposição é crucial porque permite a preservação de marcadores ambientais importantes, como metais adsorvidos na MO e nas argilas. Contudo, acessar essas informações exige técnicas geoquímicas avançadas, capazes de medir elementos em baixas concentrações (Bond et al., 2004; Guan et al., 2021; Lyons et al., 2003; Pujol et al., 2006; Zhao et al., 2016). A análise desses intervalos é essencial para identificar mudanças globais significativas, como os eventos de anoxia oceânica, que estão frequentemente associados a extinções em massa (Bond et al., 2004; Goddérís & Joachimski, 2004; Pujol et al., 2006; Carmichael et al., 2014; Sim et al., 2015; Percival et al., 2020; Zhang et al., 2023).

A Formação Irati, juntamente com outras formações do Permiano Inferior, faz parte do registro de um vasto mar epicontinental sobre o supercontinente Gondwana (Oelofsen, 1981; Oelofsen & Araujo, 1983; Rocha-Campos et al., 2019). Esta formação é composta predominantemente por siltitos e argilitos no membro inferior, e folhelhos e carbonatos no membro superior. A correlação da Formação Irati com outros registros desse mar é estabelecida pelas camadas de folhelho, que servem como um datum regional para este paleocontinente e corroboram a teoria da tectônica de placas, uma vez que ambas as formações contêm fósseis de mesossauros. Este período também é crucial para a Bacia do Paraná, onde a Formação Irati está localizada, pois marca a transição greenhouse – icehouse que leva a uma continentalização das formações posteriores (Souza et al., 2023).

Neste estudo, apresentamos um modelo das condições deposicionais da camada inferior rica em carbono orgânico da Formação Irati, na Bacia do Paraná, com base na integração de dados estratigráficos, petrográficos e geoquímicos. Através da



amostragem detalhada desse intervalo em dois testemunhos situados na porção sul da Bacia do Paraná, foram realizadas análises geoquímicas em diversas escalas, empregadas como ferramentas de quimioestratigrafia. Esta abordagem multidisciplinar não apenas oferece uma caracterização detalhada desse intervalo da Formação Irati, mas também enriquece o debate sobre os processos deposicionais e a evolução paleoambiental do Mar Irati-Whitehill. Adicionalmente, contribui para a compreensão dos fatores responsáveis pela deposição e preservação de matéria orgânica em folhelhos negros ao redor do mundo.

## 1.1 OBJETIVOS

Este trabalho teve como objetivo elucidar os fatores que desencadearam a acumulação de matéria orgânica (MO) nas formações de folhelhos ricos em carbono da Formação Irati. Para alcançar esse objetivo, foram integrados dados de descrições de fácies, informações petrográficas e dados geoquímicos e isotópicos. A investigação da evolução paleoambiental dessa formação não só visa responder a questões locais, mas também enriquecer a compreensão deposicional do extenso Mar Irati-Whitehill e da deposição de folhelhos ricos em MO em um contexto mais amplo.

## 2. ANOXIA EM BACIAS

### 2.1 TERMINOLOGIA DA CONCENTRAÇÃO DE OXIGÊNIO NO SISTEMA

A preservação de grandes quantidades de matéria orgânica (MO) em rochas como folhelhos depende de vários fatores relacionados ao ambiente sedimentar, tais como o aporte e a qualidade/fonte de MO, a taxa de sedimentação e o grau de seleção dos grãos. Um dos fatores mais importantes associados a essas condições é a oxigenação do sistema, especialmente na interface água-sedimento. Em termos gerais, a nomenclatura utilizada por biólogos baseia-se na distribuição e no comportamento faunístico de acordo com as concentrações de oxigênio. Essa classificação emprega o sufixo “aeróbico” para designar organismos que dependem de oxigênio para sobreviver, e “anaeróbico” para aqueles que não são dependentes de oxigênio. No entanto, diversas classificações das condições oxi-redutoras da água foram propostas ao longo da história, e essas classificações divergem principalmente

por definirem limites com base em grupos específicos de organismos. Tyson & Pearson, 1991 apresentaram um histórico das nomenclaturas utilizadas por biólogos e geocientistas e propuseram uma classificação dupla: uma baseada nas fácies biológicas, com o sufixo “aeróbico”, e outra baseada exclusivamente na concentração de oxigênio, com o sufixo “óxico” (Figura 1).

Bioredox facies		Environmental redox facies		
Aerobic		Oxic		2.0 mL/L
Dysaerobic		Dysoxic	moderate	1.0 mL/L
			severe	0.5 mL/L
			extreme	0.2 mL/L
Quasi-anaerobic		Suboxic		0 mL/L
Anaerobic		Anoxic		0 mL/L

$\frac{\text{O}_2}{\text{H}_2\text{S}}$   
 ↑  
 ↓

**Fig. 1** – Classificação da concentração de oxigênio com base nas fácies biooxi-redutoras e com base nas fácies ambientais oxi-redutoras, de (Tyson & Pearson, 1991; Algeo, Thomas J. & Li, 2020).

Algeo e Li (2020) apresentam uma abordagem mais completa para a terminologia da concentração de oxigênio em estudos paleodeposicionais. Neste trabalho, os autores expandem a nomenclatura das fácies redox ambientais ao incorporar limiares geoquímicos, receptores de elétrons nas reações biogeoquímicas e uma integração com a frequência temporal da anoxia. Contudo, essa classificação não inclui um critério geoquímico capaz de distinguir entre as fácies disóxicas e as fácies óxicas (fig.2). Em vez disso, essas fácies são determinadas com base em critérios paleodeposicionais, como a diversidade faunal e a intensidade da bioturbação.

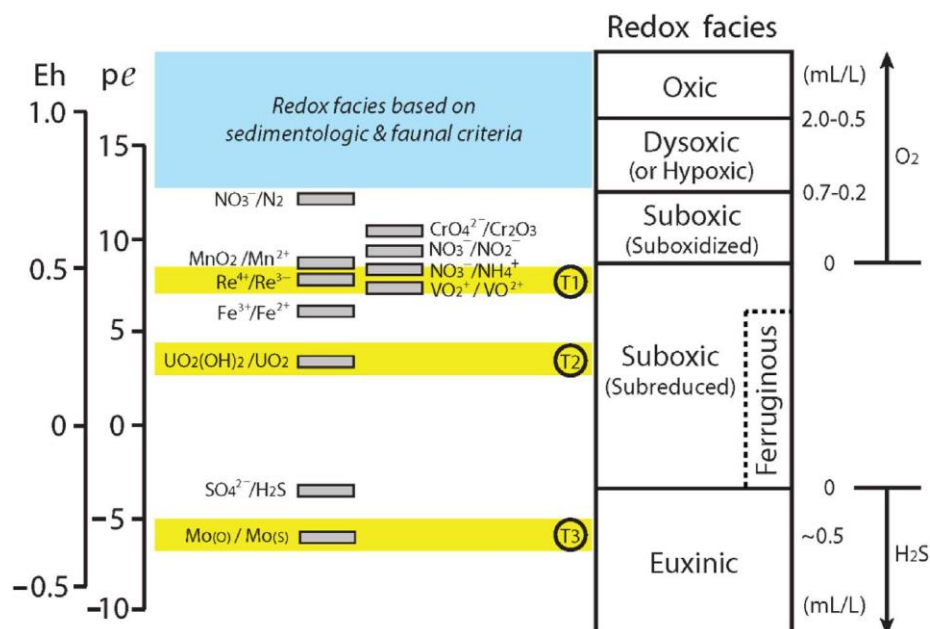


**Fig. 2** – Classificação da concentração de oxigênio no sistema e seus limiares geoquímicos. (Algeo, Thomas J. & Li, 2020)

A fácies subóxica é subdividida em duas categorias: a primeira, chamada de suboxidada, vai até a concentração zero de oxigênio; a segunda, denominada subreduzida, é caracterizada pela ausência tanto de oxigênio dissolvido quanto de H<sub>2</sub>S, mas com presença de ferro dissolvido. A fácies suboxidada inicia-se com a substituição do principal acceptor de elétrons nas reações biogeoquímicas: o O<sub>2</sub>, que passa a ocorrer em menor concentração, é substituído pelo NO<sub>3</sub><sup>-</sup>, que é convertido em N<sub>2</sub>. O limite entre a zona suboxidada e a zona subreduzida é marcado pela redução dos pares MnO<sub>2</sub>/Mn<sup>2+</sup>, Re<sup>4+</sup>/Re<sup>3+</sup>, e NO<sub>3</sub><sup>-</sup>/NO<sub>2</sub><sup>-</sup>. Além da zona subóxica subreduzida, as fácies anóxicas incluem a zona euxínica. Nesse intervalo, além da ausência de oxigênio, há a disponibilidade de H<sub>2</sub>S como principal acceptor de elétrons, liberado por bactérias redutoras de sulfato. Esse H<sub>2</sub>S possibilita a deposição de sulfetos de ferro, como a pirita, em sedimentos depositados sob essas condições.

### 3. PROXIES GEOQUÍMICOS PARA ESTUDOS PALEOAMBIENTAIS

A compreensão paleoambiental de uma formação rica em matéria orgânica depende da identificação e interpretação das informações capturadas e preservadas nos minerais e na matéria orgânica durante a deposição na bacia sedimentar. Ferramentas especializadas podem focar na fração orgânica da rocha, utilizando técnicas que avaliam tanto o potencial gerador da matéria orgânica quanto as condições deposicionais, como é o caso do uso de biomarcadores. Por outro lado, ferramentas inorgânicas analisam a rocha total ou frações específicas para revelar informações paleoambientais através da análise de razões elementares.

Goldberg & Goldberg Da Rosa, (2024) apresentam uma figura simplificada das diversas condições e suas interconexões que contribuem para a deposição de folhelhos ricos em matéria orgânica (figura 3). De forma geral, a produtividade primária e as condições redox são os principais fatores que controlam a preservação e acumulação de matéria orgânica. No entanto, esses fatores podem ser influenciados por outras condições, como as características hidrográficas que causam anoxia e o aporte de nutrientes (via fluvial ou upwelling), que aumentam a produtividade primária. Esse aumento na produtividade pode, por sua vez, reduzir as concentrações de oxigênio, criando condições redox favoráveis à preservação. Portanto, essas informações são essenciais para estudos paleoambientais de folhelhos, independentemente das ferramentas utilizadas.

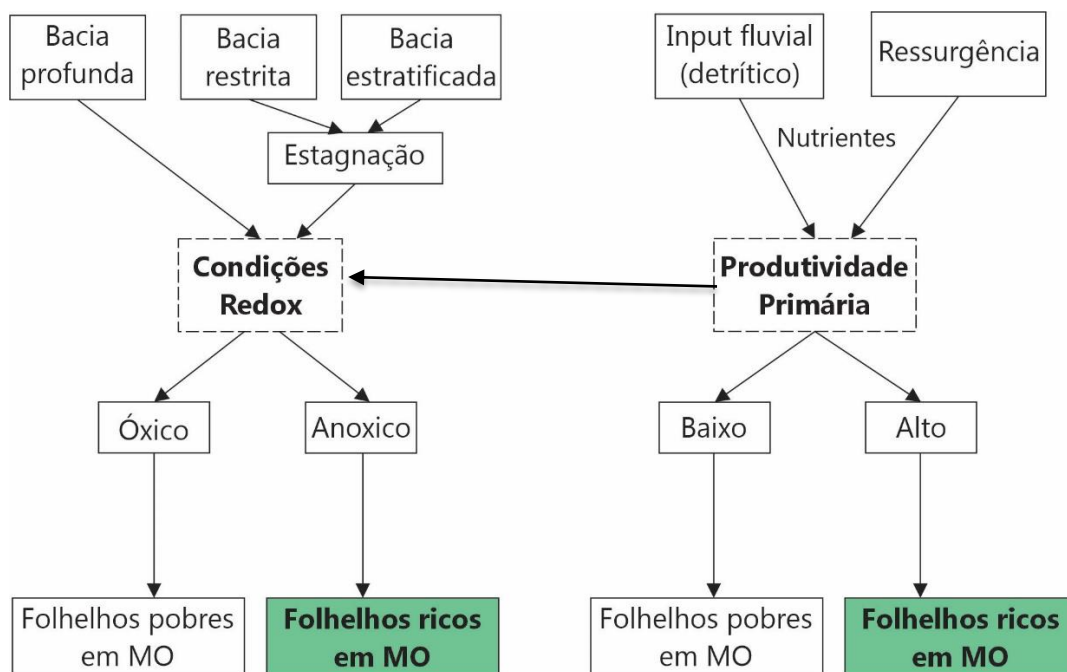


**Fig. 3** – Modelo conceitual dos controles do soterramento de matéria orgânica nos sedimentos. Extraído e traduzido de Goldberg & Goldberg Da Rosa, (2024).

No Quadro 1 estão descritas as principais razões elementares utilizadas na investigação geoquímica inorgânica para identificar os fatores que levam à deposição de folhelhos ricos em matéria orgânica (MO). No canto superior esquerdo da figura 3, são destacadas as formas de aumento dos nutrientes, como a ressurgência e o aporte fluvial, que podem ser avaliados por proxies elementares. Os **proxies de input detrítico** incluem a avaliação geoquímica da contribuição de minerais aluminossilicatos (Al%), silicatos (Si/Al) e minerais pesados como a titanita (Ti/Al) ((Algeo, Thomas J. & Maynard, 2008))

**Quadro1-** Proxies paleoambientais e suas referências

Proxy	Razão elementar	Referências
Input detrítico	Al%	Tribovillard et al., 2006
	Ti/Al	Sageman & Lyons, 2003
	Si/Al	
Produtividade primária	Cu/Al	Tribovillard, 2021
	Ni/Al	

	P <sub>ex</sub>	Schmitz et al., 1997
Condições redox	DOP	Raiswell et al., 1988
	DOPt	Algeo & Maynard, 2008;
	Fet/Al	Lyons & Severmann, 2006
	Mo, U, Cu, V...	Tribovillard et al., 2006
	V/Cr	Hatch & Leventhal, 1992;
	Ni/Co	Jones & Manning, 1994
	V/(V+Ni)	
Condições hidrográficas	Mo/TOC	Algeo & Lyons, 2006
	Cd/Mo	Sweere et al. (2016)
	Co*Mn	Sweere et al. (2016)
Salinidade	C/S	Berner & Raiswell, 1984; Wei & Algeo, 2020

Esses parâmetros são analisados em termos de empobrecimento e enriquecimento, sem valores e campos específicos definidos para avaliação. Da mesma forma, os **proxies de produtividade primária** não têm limiares de comportamento definidos e avaliam o aporte de nutrientes no sistema. Indicadores como Cu/Al e Ni/Al são utilizados porque o cobre e o níquel são frequentemente encontrados em complexos organometálicos associados à matéria orgânica (Tribovillard, 2021). O fósforo é calculado como fósforo em excesso. A normalização é feita em relação à concentração de Al<sub>2</sub>O<sub>3</sub> na amostra e à concentração média de Al<sub>2</sub>O<sub>3</sub> na crosta continental (Schmitz et al., 1997). Esse processo converte a porcentagem em massa do óxido de fósforo em fósforo em excesso, excluindo a proporção de fósforo relacionada a minerais como aluminossilicatos no sistema (ver Eq. 1).

$$\text{eq.1} \quad P_{\text{ex}} = \frac{P_2O_5}{(Al_2O_3 * 0.15)}$$

Para a avaliação das condições redox, são utilizadas diversas razões baseadas no comportamento dos elementos, onde geralmente o elemento no numerador é mais associado a condições redutoras. O grau de piritização (DOPt) é uma versão simplificada do proxy DOP, dada a importância da piritização como um indicador de condições euxínicas. No DOPt, a quantidade de ferro disponível no

sistema é estimada com base na estequiometria da porcentagem de sulfeto pertencente à pirita (ver Eq. 2). Em contraste, na fórmula original do DOP, essas porcentagens são obtidas por técnicas analíticas (Jones & Manning, 1994; Algeo, Thomas J. & Maynard, 2008).

Outra razão amplamente aceita para avaliar a oxigenação do sistema é a relação Fet/Al (Lyons & Severmann, 2006). Além dos proxies baseados em ferro, o uso de elementos sensíveis às condições redox é comum. Para essa avaliação, utiliza-se o fator de enriquecimento (EF), que indica o quanto a amostra está enriquecida em determinado elemento em comparação ao folhelho médio (AS) de Wedepohl (1971), conforme mostrado na Eq. 3. Os proxies bimetálicos propostos por Hatch & Leventhal (1992) e Jones & Manning (1994) têm seu uso desencorajado atualmente. O principal motivo é que esses proxies não são totalmente coerentes quando comparados com outros proxies, especialmente aqueles que utilizam o elemento ferro e fatores de enriquecimento.

$$\text{eq. 2: } \text{DOP}_T = S_T * (55:85/64.12)/\text{Fe}_T$$

$$\text{eq.3: } X_{EF} = (X_{\text{sample}}/A_{\text{sample}}) / (X_{AS}/A_{AS})$$

Os indicadores paleohidrográficos são de grande importância, pois podem, por si só, promover condições mais redutoras na bacia sedimentar. Como ilustrado na figura, bacias que podem levar à anoxia incluem bacias restritas, bacias profundas e bacias estratificadas (Demaison & Moore, 1980). A bibliografia frequentemente usa o termo "silled basin" para se referir a bacias com algum tipo de restrição, mas aqui utilizaremos um termo mais genérico (Demaison & Moore, 1980). As bacias restritas, como o Mar Negro, são um exemplo atual significativo. Elas provocam anoxia devido a um balanço hídrico positivo, onde o aporte fluvial é maior que o escoamento. Isso resulta em uma diferença significativa de salinidade (haloclima), que separa a zona oxigenada da zona anóxica. As bacias profundas, por sua vez, apresentam uma estratificação permanente. A matéria orgânica (MO) que se desenvolve na superfície é decomposta ao longo da coluna d'água, sequestrando e reduzindo o oxigênio das camadas mais profundas.

Para identificar ambientes como esses, são utilizados proxies com

elementos que têm afinidade com a matéria orgânica e com ambientes anóxicos, como Mo e Cd. A razão Cd/Mo também permite a distinção entre ambientes anóxicos restritos e aqueles com algum componente de ressurgência. Além disso, o proxy de salinidade está diretamente relacionado ao aporte fluvial, que é um dos gatilhos para a paleoprodutividade e, conseqüentemente, para a anoxia. O proxy C/S, que utiliza o carbono orgânico total e o enxofre total, só pode ser aplicado em amostras com mais de 1% de COT, o que dificulta a distinção entre ambientes marinhos e ambientes salobros (Bernier & Raiswell, 1984). Proxies alternativos, como B/Ga e Sr/Ba, são considerados melhores para a investigação da paleosalinidade (Wei & Algeo, 2020).

Os proxies de condições oxi-redutoras, condições hidrográficas e salinidade possuem limites definidos pelos autores mencionados no Quadro 1. Esses limites foram agrupados e estão sumarizados na Figura 4.

REDOX			HIDROGRAFIA	SALINIDADE		
DOPt	Fet/Al	V/ (V+Ni)	Mo/ COT	Cd/ Mo	Co* Mn	C/S
óxico 0.3	óxico <0.5-0.6	óxico 0.60	não restrito 35	ressurgencia 0.1	0.4	marinho 2
subóxico 0.6	0.7	subóxico 0.84	moderadamente restrito 15	restrito		salobra 10
euxínico	euxínico	euxínico	extremamente restrito			doce

**Fig. 4** – Resumo dos limites dos proxies redox, de condições hidrográficas e de salinidade segundo as referências do quadro 1.

#### 4 BACIA DO PARANÁ

A Bacia do Paraná é uma bacia intracratônica de idade Paleozoica situada na região meridional da América do Sul, abrangendo cerca de 1.000.000 km<sup>2</sup> no Brasil e mais 500.000 km<sup>2</sup> em países vizinhos como Argentina, Uruguai e Paraguai,



formando parte da Bacia Chaco-Paraná (Fig.1) (Schneider et al., 1974). A sedimentação nessa bacia é predominantemente controlada por ciclos tectono-eustáticos, que dividem a sua estratigrafia em nas supersequências: Rio Ivaí (Ordoviciano-Siluriano), Paraná (Devoniano), Gondwana I (Carbonífero - Triássico), Gondwana II (Triássico), Gondwana III (Jurássico – Cretáceo) e Bauru (Cretáceo Superior) (Milani & Ramos, 1998) (Figura 5 e 6).

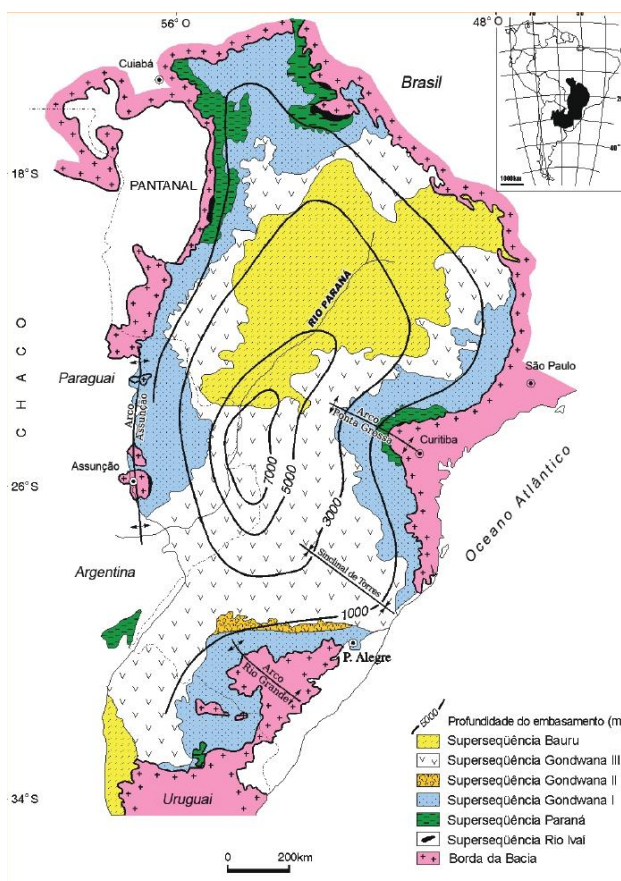


**Fig. 5** – Bacia do Paraná agrupada a partir de suas supersequências, extraído de (Milani, E. et al., 2007)

A Formação Irati, foco deste estudo está localizada na Supersequência Gondwana I, que abrange os sedimentos depositados entre o Carbonífero e o Triássico. Na base dessa supersequência encontra-se o Grupo Itararé, composto por depósitos glácio-marinhos e glacio-lacustres. Sobre este, o Grupo Guatá é caracterizado por depósitos de plataforma e pelo desenvolvimento de turfeiras, refletindo um período transgressivo da bacia associado à deglaciação. No topo da supersequência, o Grupo Passa Dois registra a transição permiana de Greenhouse para Icehouse, com sedimentos marinhos do Mar epicontinental Irati-Whitehill na base

e depósitos continentais, incluindo sedimentos fluviais e eólicos, no topo (Holz et al., 2010; Souza et al., 2023).

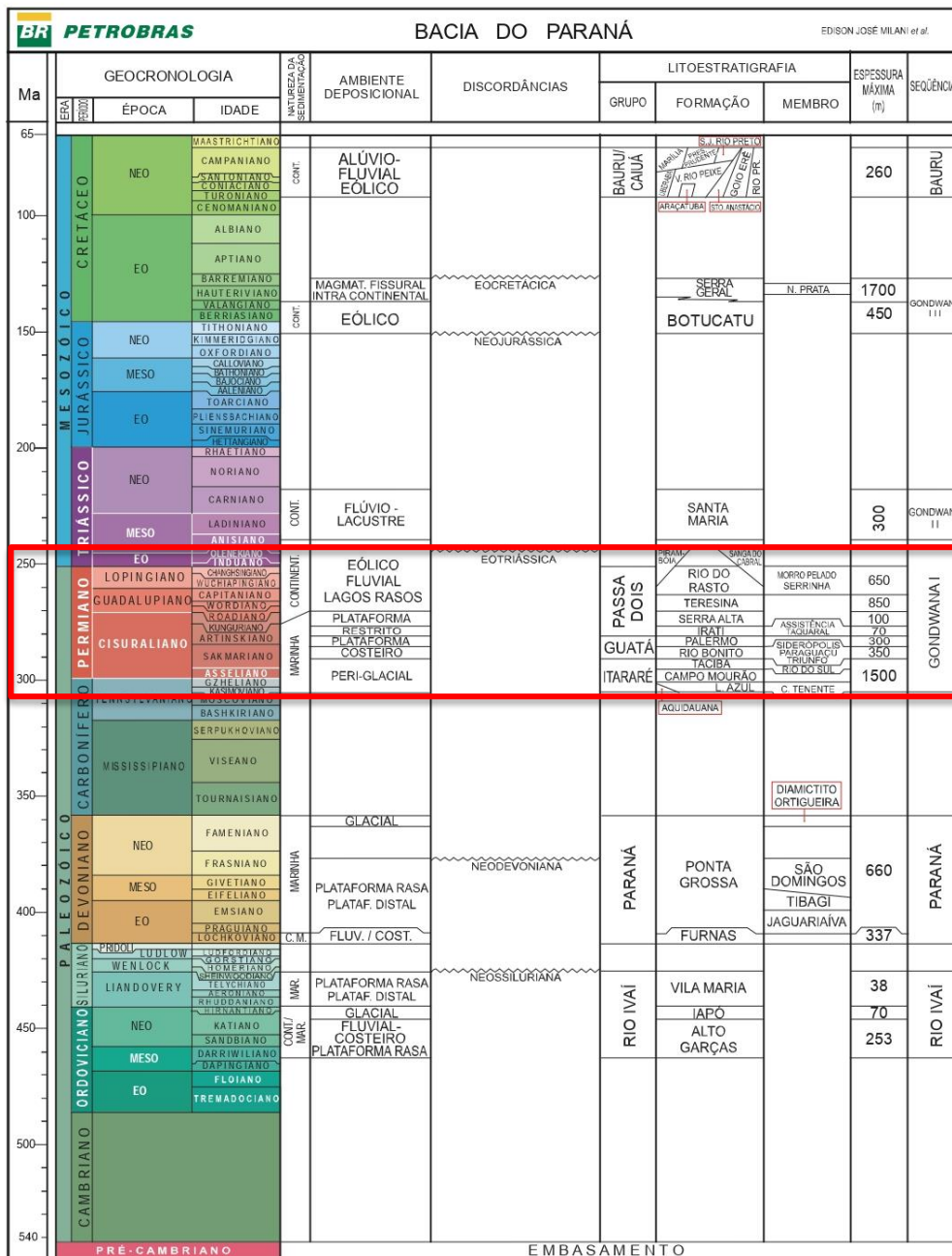


**Fig. 6 -** Carta cronoestratigráfica da Bacia do Paraná. Superseqüência Gondwana I em destaque no retângulo vermelho (modificado de Milani, Edison José et al., 2007).

## 4.1 FORMAÇÃO IRATI

### 4.1.1 Idade

A Formação Irati, base do grupo passa dois, tem ampla ocorrência na Bacia do Paraná e foi depositada no Permiano Inferior. Dados palinológicos posicionam essa formação dentro da palinozona *Lueckisporites virkkiae* (Souza & Marques-Toigo, 2005; Souza, 2006). Datações radiométricas por U-Pb em zircão indicam idade Kunguriana para a formação. Como as idades obtidas em São Matheus do Sul, PR, por U-Pb SHRIMP,  $279,9 \pm 4,8$  Ma e  $280,0 \pm 3$  Ma (Rocha-Campos et al., 2019),  $278,40 \pm 2,2$  Ma (Santos et al., 2006), e  $277,26 \pm 0,62$  Ma por IDTIMS (Bastos et al., 2021). Entretanto, datações feitas na porção sul da bacia (Pedras Altas, RS) apontam idades mais jovens, como  $275,75 \pm 0,29$  Ma por U-Pb em zircão por IDTIMS.

### 4.1.2 Litologia

O ambiente paleodeposicional dessa formação é caracterizado por uma rampa com direção nordeste-sudoeste e inclinação para o sul que marca uma heterogeneidade litofaciológica de sul para norte (Hachiro, 1997; Araújo, 2001). Onde no sul, predominam as fácies siliciclásticas e relativamente mais profundas, enquanto no norte, predominam rochas carbonáticas e, ocasionalmente, evaporíticas. A Fm. Irati é dividida ainda em dois membros, que separam dois momentos deposicionais diferentes. No Membro Taquaral, de base ocorrem siltitos e argilitos sem a presença de matéria orgânica (Araújo, 2001; Holz et al., 2010). O Membro Assistência, no entanto, parece ser homogêneo na porção sul com duas sequências de quarta ordem com camadas de carbonato marcando a regressão máxima e folhelho ricos em matéria orgânica apontando a transgressão máxima (Araújo, 2001; Milani, Edison José et al., 2007; Holz et al., 2010; Goldberg & Humayun, 2016). Comparativamente o folhelho inferior apresenta maior concentração de carbono orgânico total chegando a 25% enquanto o folhelho superior chega a até 15%.

### 4.1.3 Entendimento paleoambiental

O entendimento paleoambiental da deposição do Membro Assistência é que suas fácies têm como principal controlador a variação do nível do mar. O Mar Irati-Whitehill se colocava no continente Gondwana como um mar interior que por vezes se comunicava com as águas do Oceano Pantalassa (Araújo, 2001). A evolução desse membro foi investigada a partir de técnicas de geoquímica orgânica e isotópicas por Bastos et al., 2021. Esse autor evidencia que o membro assistência inicia sua deposição em um paleoambiente hipersalino, que em direção ao topo recebe influxos terrestres e marinhos que favorecem a estratificação da coluna d'água. A redução da salinidade é acompanhada por picos de produtividade primária que levam a deposição de elevados teores de carbono orgânico total (até 25%) (folhelho inferior). Para o topo ocorre o reestabelecimento de condições óxicas- subóxicas que levam a uma redução no conteúdo de COT. Essas observações feitas por Bastos também são encontradas em estudos pontuais dos folhelhos inferior e superior na região de Amaral Machado, na porção norte da bacia no estado de São Paulo.

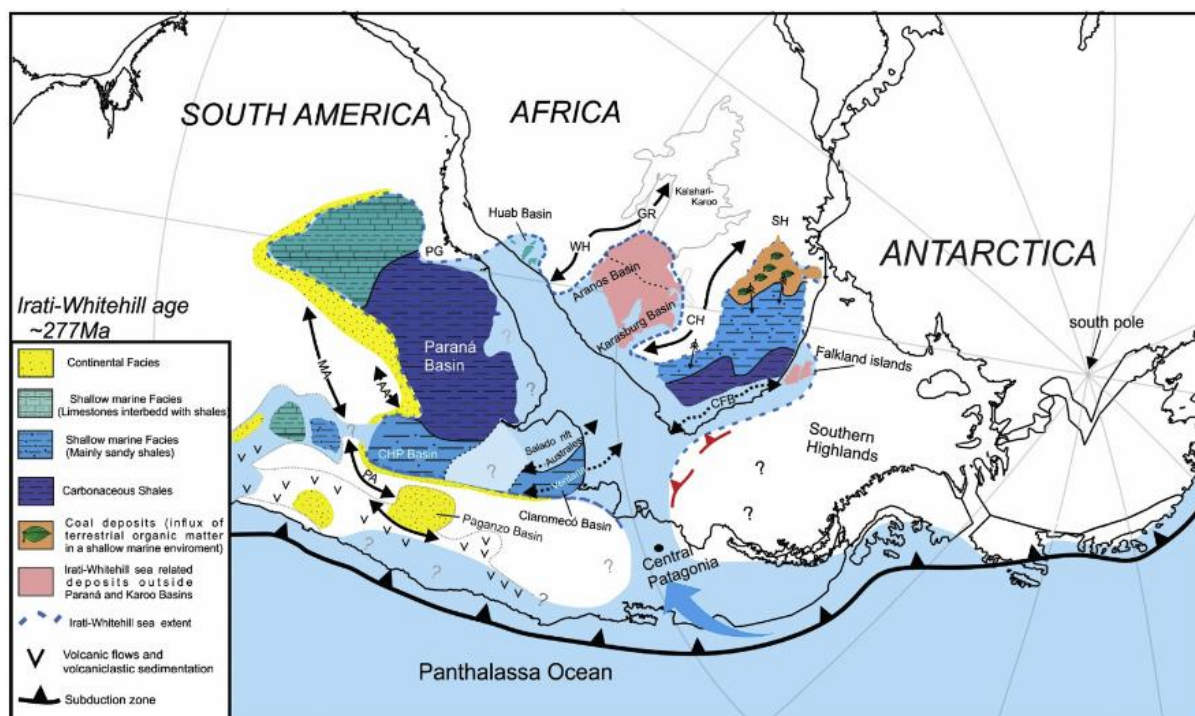


**Fig. 7** – Reconstrução paleogeográfica do Mar Irati-Whitehill, extraído de (Bastos et al., 2021)

## 5 MATERIAIS E MÉTODOS

Este estudo foi conduzido na porção sul da Bacia do Paraná, especificamente na região de Candiota no estado do Rio Grande do Sul. Foram perfurados dois poços, denominados HV-54-RS e SC-15-RS (representado pela caixa laranja na Fig 8C). O Serviço Geológico do Brasil (CPRM) concedeu acesso aos testemunhos para a realização das descrições e coletas de amostras. O intervalo analisado compreende a porção basal da Fm. Irati, do membro Taquaral até a porção intermediária do Membro Assistência. Sendo de 32 metros de espessura no poço HV-54-RS (coordenadas UTM 226000mN 648201mE) e 38 metros no poço SC-15-RS (coordenadas UTM 239103mN 6486005mE).

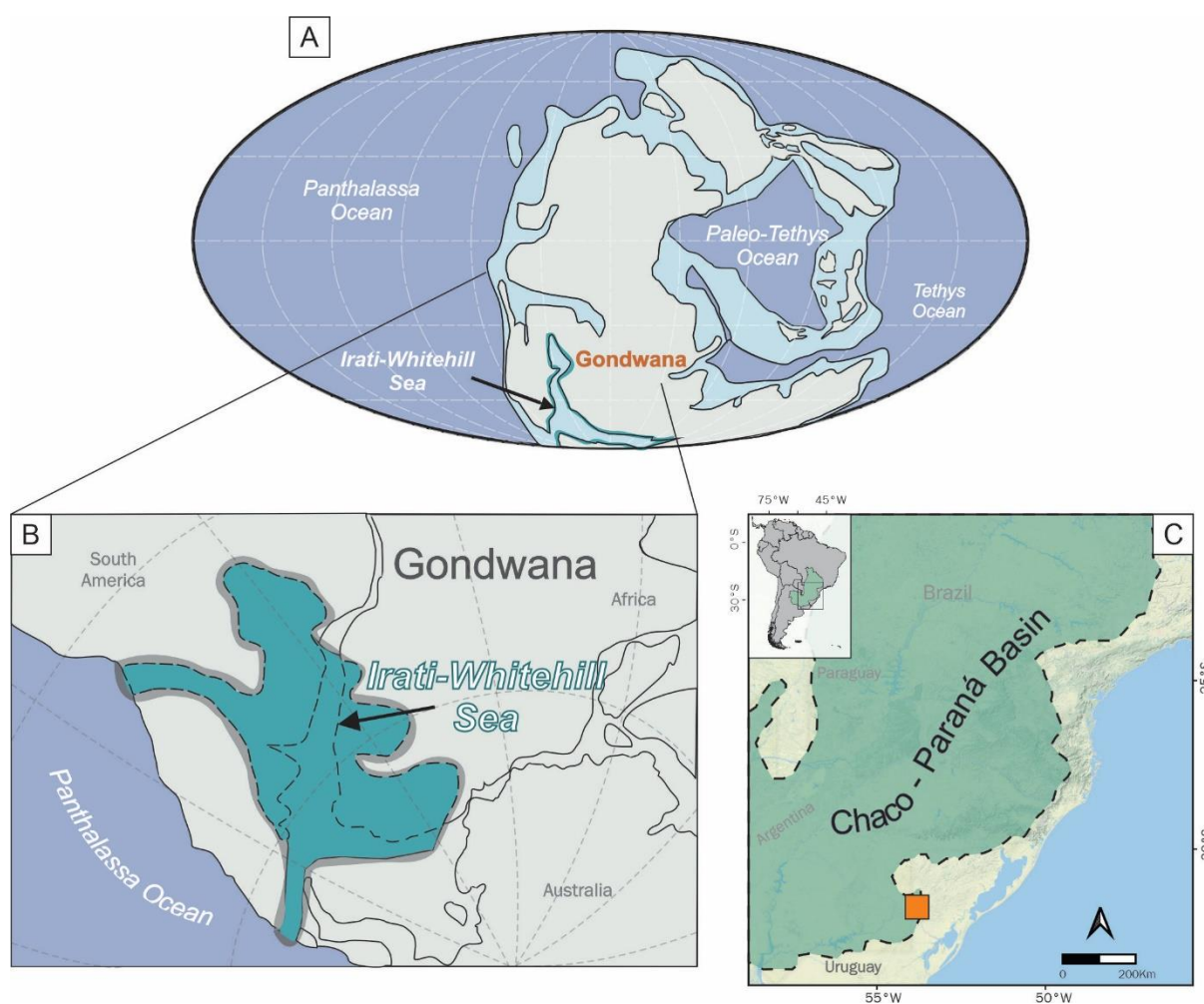


**Fig. 8** – Reconstrução global do Permiano Inferior (Scotese, 2016) (A) com a reconstrução paleogeográfica do Mar Irati- Whitehill (B), modificado após Bastos et al. (2021), mostrando a localização da área de estudo (C).

A metodologia seguida constituiu-se da caracterização litológica e texturais, por meio de descrição dos testemunhos dos quais foram coletadas 16 amostras para análise petrográfica (5 lâminas do poço HV-54 e 11 do poço SC-15). Foram ainda coletadas 55 amostras do folhelho inferior, ricos em matéria orgânica, para análises geoquímicas (20 do poço HV-54 e 35 do poço SC-15). Essas amostras foram caracterizadas por difração de raios X (DRX), fluorescência de raios X (FRX), carbono orgânico total (TOC), enxofre total, elementos redox-sensíveis como urânio (U), molibdênio (Mo) e cádmio (Cd) (via ICP-MS), além de isótopos de carbono orgânico.

## 6 SÍNTESE DOS RESULTADOS E INTERPRETAÇÕES

A partir da integração das descrições de fácies e análises petrográficas com a geoquímica detalhada, foi possível caracterizar o folhelho inferior da Formação Irati. Essa integração possibilitou remontar a evolução paleoambiental e a identificação dos potenciais fatores que contribuíram para o acúmulo e preservação significativa de matéria orgânica (MO).

- As associações de fácies permitiram estimar a profundidade paleobatimétrica dos testemunhos: o SC-15, a leste, possui fácies mais proximais, com carbonatos e evidências de exposição subaérea; o HV-54, a oeste, apresenta litologias indicativas de um ambiente mais distal.
- Os padrões quimioestratigráficos revelam diferentes evoluções de anoxia entre os testemunhos: SC-15 apresenta intervalos pré-orgânicos e de incremento orgânico, enquanto HV-54 já mostra altos níveis de TOC desde o início, sem transições geoquímicas significativas.
- O testemunho SC-15, em águas mais rasas, exibe um aumento gradual de TOC, enquanto HV-54, em águas mais profundas, não apresenta mudanças significativas nos proxies quimioestratigráficos, sugerindo maior estabilidade nas condições ambientais.
- Durante os Intervalos de Estabilidade Orgânica, o TOC permaneceu elevado (>10% no SC-15 e entre 5-10% no HV-54), com alta produtividade primária indicada por proxies como Cu/Al, Ni/Al e Pex.

- SC-15 apresentou salinidade consistentemente baixa nos intervalos de estabilidade orgânica, enquanto HV-54 manteve indicadores de água salobra, correlacionados com picos de produtividade.
- Enriquecimento de molibdênio e urânio nos intervalos de estabilidade orgânica indica condições anóxicas a euxínicas, enquanto DO<sub>Pt</sub> sugere condições oxigenadas devido a baixas concentrações de sulfato dissolvido.
- Indicadores como Mo/TOC e Cd/Mo sugerem um ambiente restrito, enquanto Co/Mn indica ressurgências intermitentes, revelando a complexidade do ambiente deposicional da bacia.
- As amostras ricas em matéria orgânica do estudo mostram comportamento similar ao da Bacia de Cariaco, sugerindo um ambiente deposicional controlado por ressurgências ocasionais e influxo de água doce.
- A entrada de água doce, possivelmente responsável pela redução de salinidade e aumento da produtividade bacteriana, ainda precisa de mais estudos para determinar sua origem.
- Caracterizados por TOC inferior a 5%, esses intervalos mostram aumento no aporte detrítico e redução nos proxies de produtividade e condições redox, com mudanças abruptas no SC-15 e graduais no HV-54.

## CAPITULO II ARTIGO

1 ARTIGO SUBMETIDO EM INTEIRO TEOR

### **Geochemical Insights into Paleoenvironmental Influences on Organic-Rich Shale Deposition in the Irati-Whitehill Sea, Southern Paraná Basin**

Jhenifer Caroline da Silva Paim<sup>1</sup>; Juliana Charão Marques<sup>1</sup>; Karin Goldberg<sup>2</sup>; Diogo Pompeu Moraes<sup>3</sup>

<sup>1</sup>Isotopic Geology Laboratory, Institute of Geosciences, Federal University of Rio Grande do Sul (UFRGS), 91501-970, Porto Alegre, Brazil

<sup>2</sup>Department of Geology, Kansas State University, Manhattan, USA

<sup>3</sup>Applied Analytical Chemistry Center, Institute of Chemistry, Federal University of Rio Grande do Sul (UFRGS), 91501-970, Porto Alegre, Brazil

E-mail addresses: jheniferpaimufrgs@gmail.com (Jhenifer Caroline da Silva Paim)

#### **HIGHLIGHTS:**

- Evolution of anoxia in the Irati-Whitehill Sea is not locally homogeneous.
  - The process appears to be associated with paleobathymetry.
- OM-rich interval is correlated with salinity decrease and high primary productivity.
- The microbial bloom triggered an anoxic environment that led to anoxia and euxinia.

#### **ABSTRACT**

The Irati-Whitehill Sea was a vast epicontinental sea on the paleocontinent Gondwana during the Lower Permian. In Brazil's Paraná Basin, the Irati Formation represents this ancient sea. In the southern part of the basin, two intervals of organic-rich shales are identified, with the lowermost one displaying the highest levels of total organic carbon (TOC). To elucidate the conditions that triggered organic matter (OM) accumulation in the lower shale, this study integrates facies and petrographic descriptions with geochemical and isotopic data from two wells in the southern Paraná Basin. The intervals were subdivided based on the paleoenvironmental evolution of anoxia in a



lacustrine or restricted marine environment, which allowed the deposition of organic-rich shales. The studied interval begins with deposition in a saline environment with low organic matter concentration (pre-organic interval), where salinity gradually decreases, primary productivity increases, and anoxia intensifies, culminating in an increase in organic content (organic increment interval). The highest concentration of organic matter (15% TOC) occurs alongside low salinity and high primary productivity, and is well-marked by anoxic to euxinic conditions (organic stability interval). This suggests an environment where freshwater influx triggered a microbial bloom, leading to oxygen depletion and OM preservation. After this peak in OM accumulation, the environment became oxygenated, with regular detrital input and low primary productivity in the low-organic interval. Similar conditions have been observed in other basins worldwide, such as the Cariaco Basin, a restricted basin with episodic upwellings considered as a low-frequency temporal redox system. Therefore, the Irati-Whitehill Basin parallels the dynamics observed in the Cariaco Basin, functioning as a restricted basin with episodic freshwater input.

**KEYWORDS:** Organic-rich shales, paleoenvironmental, chemostratigraphy, anoxic, primary productivity, salinity

## 1. Introduction

The study of sedimentary basins has become increasingly interdisciplinary. Although traditional stratigraphic techniques are fundamental for the geological understanding and evolution of sedimentary successions, fine-grained siliciclastic rocks, such as organic-rich shales, require complementary approaches that allow access to information beyond lithological descriptions (LaGrange et al., 2020). For instance, trace elements adsorbed onto clays and organic matter during deposition capture and store essential information about the depositional paleoenvironment. The detailed application of chemostratigraphy, combined with advanced analytical techniques such as inductively coupled plasma mass spectrometry (ICP-MS) and X-ray diffraction (XRD), allows for the precise characterization of the evolution of the depositional paleoenvironment (Lyons et al., 2003; Bond et al., 2004; Pujol et al., 2006; Zhao et al., 2016; Guan et al., 2021), providing insights into the origin, preservation, and distribution of organic matter, as well as revealing subtle changes in redox conditions and sedimentation regimes over time (Berner & Raiswell, 1984; Jones & Manning, 1994; Murphy et al., 2000; McArthur, J. et al., 2008; Algeo, T.J. & Tribovillard, 2009; Sweere et al., 2016; McArthur, J. M., 2019). Studies using this approach have allowed for a more comprehensive understanding of organic-rich shale intervals in basins such as Sichuan, Songliao, and the Lower Yangtze region in China (Zhao et al., 2016; Guan et al., 2021; Shu et al., 2021; Zhang et al., 2023). Additionally, they are the primary tool for understanding the causes of oceanic anoxia events and tracing these processes across continents, such as those that occurred between the Frasnian and Famennian stages (Bond et al., 2004; Godd ris & Joachimski, 2004; Pujol et al., 2006; Carmichael et al., 2014; Sim et al., 2015; Percival et al., 2020; Zhang et al., 2023) and during the Cretaceous (Brumsack, 1986; Jenkyns, 2010; McArthur, J. M., 2019). On a larger scale, 3D mapping of these geochemical proxies can indicate potential 'sweet spots' for shale gas exploration (Zhai et al., 2019; Wang et al., 2022), offering a powerful tool for the oil and gas industry in identifying zones of higher potential.

Although chemostratigraphy has already established itself as an important tool for the study of sedimentary basins around the world, its potential can be further explored in case studies like that of the Irati-Whitehill Sea. This vast epicontinental sea covered part of western Gondwana during the Lower Permian, leaving a sedimentary

record of up to 70 meters, composed of siltstones to mudstones and in the upper member carbonates interbedded with shales (Milani, Edison José et al., 2007; Holz et al., 2010). During this period, two intense anoxia events occurred, resulting in the deposition of organic-rich shales (Milani, Edison José et al., 2007; da S. Ramos et al., 2015). The lower black shale layer stands out with up to 20% total organic carbon; this high hydrocarbon-generating potential has already been explored in Brazil for shale gas extraction. Additionally, these anoxic events also led to the preservation of Mesosaurus fossils, which can be correlated on a global scale in the Paraná (Brazil), Chaco (Argentina and Uruguay), and Karoo (Namibia) basins. The correlation of this fossiliferous black shale layer not only served as evidence for the theory of plate tectonics but also contributed to global paleogeographic reconstruction. The significant preservation of organic matter in this sea, as in other locations around the world, remains a topic of debate. The relationship between primary productivity and anoxia highlights the importance of using geochemical tools to better understand these processes (Goldberg & Goldberg Da Rosa, 2024).

The Irati Formation are the deposits of the ancient Irati-Whitehill Sea in the Paraná Basin, Brazil. Although it holds great economic and scientific importance, the detailed understanding of this extensive body of water, especially the organic-rich intervals, is still limited. Studies investigating the stratigraphic evolution of the Irati have primarily focused on organic geochemistry tools ((da S. Ramos et al., 2015; Martins, Laercio Lopes et al., 2020; Nascimento et al., 2021). Bastos and collaborators (2021) presented an integration of stratigraphy with organic and isotopic geochemical data, enriching the analysis. Regarding the integration of stratigraphic data with inorganic geochemistry, studies such as that of Goldberg & Humayun (2016) demonstrate the importance of this approach and reinforce the significance of multidisciplinary analyses for a deeper understanding of the depositional and paleoenvironmental conditions of the Irati Formation.

In this study, we present a model of the depositional conditions of the lowermost, TOC-rich organic shale layer of the Irati Formation in the Paraná Basin, based on an integration of stratigraphic, petrographic, and geochemical data. Through detailed sampling of this interval in two cores located in the southern Paraná Basin, geochemical analyses were conducted at various scales, including major elements, trace elements, total organic carbon, and organic carbon isotopes, as tools for chemostratigraphy. This multidisciplinary approach not only provides a detailed

characterization of this interval of the Irati Formation but also enriches the debate on the depositional processes and paleoenvironmental evolution of the Irati-Whitehill Sea. Furthermore, it contributes to the understanding of the factors responsible for the deposition and preservation of organic matter in black shales around the world.

## 2. Geological setting

The Paraná Basin is a Paleozoic intracratonic basin located in the southern portion of South America, covering approximately 1,000,000 km<sup>2</sup> within Brazil and an additional 500,000 km<sup>2</sup> in neighboring countries such as Argentina, Uruguay, and Paraguay within the Chaco-Paraná Basin (Fig. 1) (Schneider et al., 1974). The primary mechanism controlling sedimentation in the Paraná Basin is tectono-eustatic cycles, which subdivide the stratigraphy into six supersequences (Milani, Edison J. & Ramos, 1998).

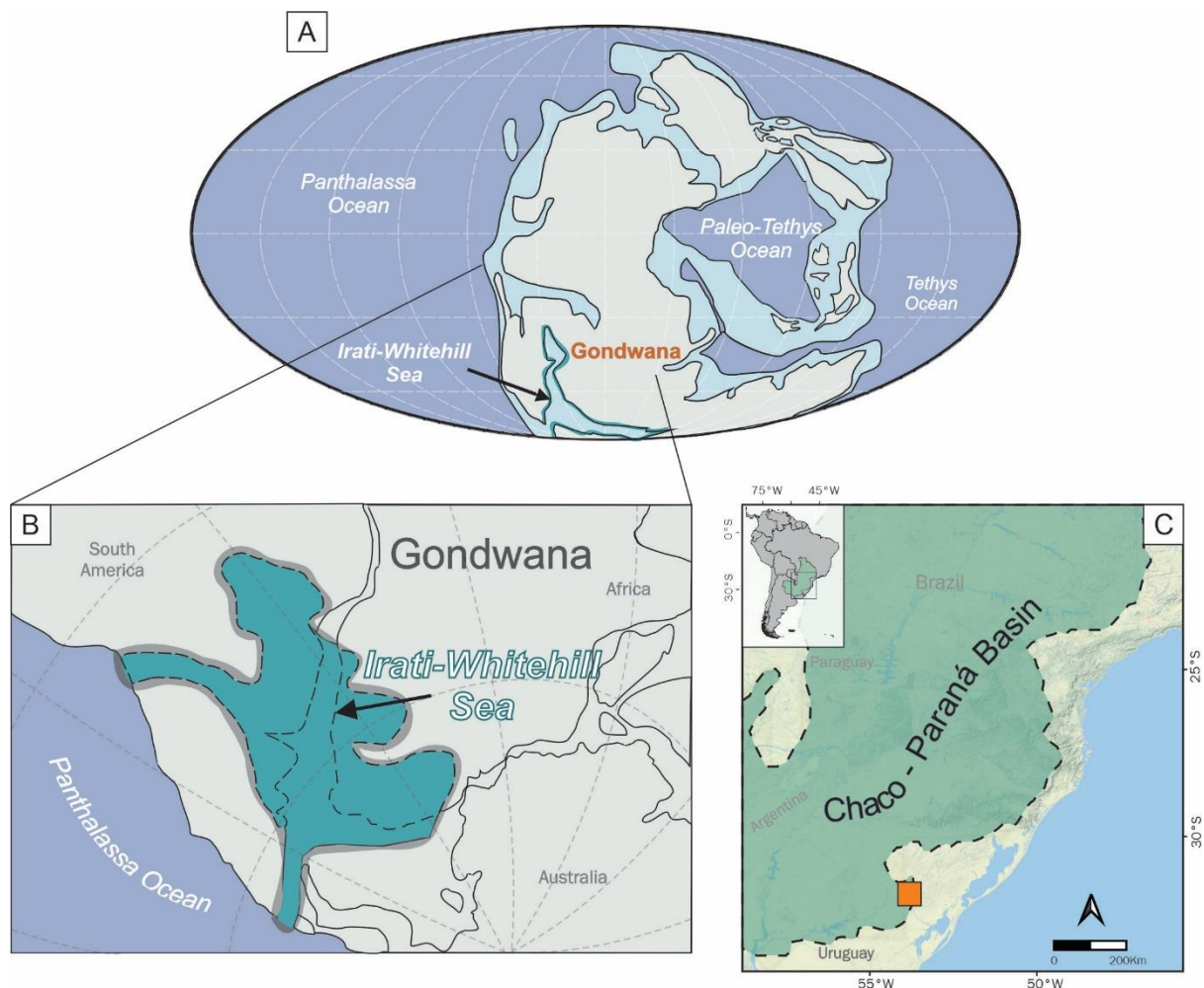


Fig.1 - Global Reconstruction of the Late Permian (Scotese, 2016) (A) with the paleogeographic reconstruction of the Irati-Whitehill Sea (B), modified after Bastos et al. (2021), showing the location of the investigated area (C).

The Gondwana I supersequence is divided into three groups, encompassing sediments deposited from the Carboniferous to the Triassic. The Itararé Group is at the base of the supersequence and consists of glacial-marine and glacial-lacustrine deposits. Next, the Guatá Group is characterized by platform deposits with the development of peat bogs, representing a transgressive phase of the basin caused by deglaciation. At the top of the supersequence, the Passa Dois Group marks the Permian Greenhouse-Icehouse transition, with the deposition of marine sediments in the Irati-Whitehill epicontinental sea at the base, transitioning to continental deposits with fluvial and aeolian sediments at the top (Holz et al., 2010; Souza et al., 2023).

The Irati-Whitehill Sea was a vast epicontinental sea that developed on the supercontinent Gondwana during the Lower Permian (Fig.1C). The global correlation of records from this sea is supported by diagnostic features such as the thick black shale layers and the presence of *Mesosaurus* fossils, which reinforced the theory of continental drift. The formations that document this large body of water include the Irati Formation in the Paraná Basin, the Whitehill Formation in the Karoo, Huab, and Karasburg Basins of Africa (Oelofsen, 1981; Oelofsen & Araujo, 1983) the San Miguel and Tacuary Formations in Paraguay and the Mangrullo Formation in Uruguay, the latter two located in the Chaco-Paraná Basin (Rocha-Campos et al., 2019).

The Irati Formation has a wide occurrence in the Paraná Basin. Its Lower Permian is indicated by palynological data that place it within the *Lueckisporites virkkiae* palynozone (Souza & Marques-Toigo, 2005; Souza, 2006). Radiometric U-Pb dating on zircon suggests a Kungurian age for the formation. Ages obtained in São Mateus do Sul, Parana State, through U-Pb SHRIMP, indicate  $279.9 \pm 4.8$  Ma and  $280.0 \pm 3$  Ma (Rocha-Campos et al., 2019), and  $278.40 \pm 2.2$  Ma (Santos et al., 2006), as well as  $277.26 \pm 0.62$  Ma by IDTIMS (Bastos et al., 2021). However, ages obtained in the southern portion of the basin (Pedras Altas, Rio Grande do Sul State) indicate younger ages, such as  $275.75 \pm 0.29$  Ma by U-Pb zircon IDTIMS (Cagliari et al., 2022).

This formation was deposited in a northeast-southwest oriented, southward-dipping ramp, with a lithofacies heterogeneity from south to north. In the

south, siliciclastic and relatively deeper-water facies predominate, while in the north, carbonate and occasionally evaporitic rocks are more common. The Irati Formation is divided into two members: Taquaral and Assistência. The Taquaral Member, composed of gray to black siltstones and shales, was deposited in a shallow marine environment with good water circulation (Holz et al., 2010). Bastos et al., (2021) classify this member as the first (Stage I) of five developmental stages in the formation, characterized by deposition in a water-renewed environment with terrestrial organic matter input and normal salinity.

The Assistência Member, comprising shales and organic-rich shales interbedded with carbonates, was deposited in an environment with limited connection to the waters of the Panthalassa Ocean (Araújo, 2001). Its facies are controlled by sea level variations, resulting in the deposition of organic-rich shales in anoxic environments during transgressive phases (Araújo, 2001; Milani, Edison José et al., 2007; Holz et al., 2010; Goldberg & Humayun, 2016). In the southern portion, two fourth-order sequences are distinctly marked, both beginning with the deposition of carbonate facies in lowstand systems tracts and culminating in the deposition of organic-rich shales in transgressive systems tracts (Xavier et al., 2018).

Stage II of basin evolution, as described by Bastos et al., (2021), highlights a change in depositional environment between the two members. This stage is represented by a hypersaline depositional paleoenvironment, which towards the top receives terrestrial and marine influxes that favor water column stratification. Higher total organic carbon (TOC) levels (up to 25%) are observed at the base of Stage III, pointing to strong anoxia. During this period, there was also high primary productivity and proliferation of prokaryotic organisms. Towards the top, oxic-suboxic conditions were reestablished, leading to a reduction in TOC content. Finally, the subsequent stages indicate a return to high salinity (Stage IV), which evolves into another period of intense anoxia (Stage V) (Bastos et al., 2021).

### **3. Methods**

#### **3.1 Study site and samples**

This study was conducted in the southern portion of the Paraná Basin, within the basal section of the Assistência Member of the Irati Formation. Two wells (HV-54-RS and SC-15-RS) were drilled in the southern part of the Paraná Basin in Rio

Grande do Sul State (orange box in Fig. 1C). Access to the cores for description and sampling was provided by the Geological Survey of Brazil (CPRM). The studied interval is 32 meters thick in core HV-54-RS (UTM coordinates 226000N 648201E) and 38 meters thick in core SC-15-RS (UTM coordinates 239103N 6486005E).

Based on lithological and textural characteristics, 16 samples were collected for petrographic analysis (5 thin sections from core HV-54 and 11 from SC-15) and 55 samples of organic-rich shales for geochemical analyses (20 from HV-54 and 35 from SC-15). These samples were characterized using X-ray diffraction (XRD), X-ray fluorescence (XRF), total organic carbon (TOC), total sulfur, redox-sensitive elements such as uranium (U), molybdenum (Mo), and cadmium (Cd) (via ICP-MS), and organic carbon isotopes.

### **3.2 Core description**

Facies analysis involved a detailed description at a 1:50 scale of approximately 70 meters of the Irati Formation section, distinguishing attributes such as color, grain size, grain composition, bed geometry, sedimentary structures and degree of bioturbation. The identified facies were further grouped into facies associations, which aided in determining the depositional processes and paleoenvironmental conditions.

### **3.3 Petrographic Analysis**

Petrographic analysis involved the description and quantification of features in 16 thin sections using a petrographic microscope. The description included textural and compositional aspects of detrital and diagenetic constituents, as well as pore types. Descriptive data and photomicrographs were collected and stored using Petroledge®.

### **3.4 X-ray Diffraction**

X-ray diffraction (XRD) analysis was conducted at the Petroleum Institute (IPR-PUCRS). Measurements were performed using a Bruker D8 Advance diffractometer, equipped with a copper tube, operating at 40 kV voltage and 30 mA

current. The scanning for the total sample ranged from 2Theta 3° to 70°, with a step size of 0.015° and a counting time of 0.2 seconds. The interpretation of the diffractograms was carried out using DIFFRAC.EVA V3.1 software, based on the PDF-2013 database (Powder Diffraction File – 2013).

The clay fraction of the samples was separated to differentiate these mineral phases. For each sample, three analyses were conducted: (1) the oriented sample using the smear method, (2) the sample solvated with ethylene glycol for 15 hours in a vacuum desiccator, and (3) the sample heated to 490 °C for 5 hours. The scanning of the oriented samples followed the same parameters as the total sample. For the analyses of readings 2 and 3, the scanning range was from 2Theta 3° to 35°, with the same step size and counting time.

### **3.5 Total carbon and sulfur content**

The samples selected for geochemical characterization underwent preparation, including drying at 60°C in an oven and grinding to 60 mesh. These samples were then sent to the Petroleum Institute IPR-PUCRS for Total Organic Carbon (TOC) and sulfur (S) analyses. Prior to analysis, the samples were treated with HCl to remove any carbonate residues, then washed five times and dried again at 60°C for 24 hours. TOC analysis was performed using a non-dispersive TRUSPEC/LECO analyzer, equipped with an infrared detector, which combusts the samples in an oxygen atmosphere at 950°C. For sulfur quantification, a LECO SC-632 elemental analyzer was used, where samples are burned at 1350°C under 1 atm and measured with an infrared detector.

### **3.6 Major and redox-sensitive element analysis**

The samples, ground to 60 mesh for geochemical analysis, were sent to ActLabs, a commercial laboratory, for major element analysis using X-ray fluorescence (XRF). For the determination of redox-sensitive elements (V, Cr, Co, Ni, Cu, Zn, Mo, Cd, Sn, Tl, Pb, U), the samples were processed using the facilities at the Applied Analytical Chemistry Center (NUQA-UFRGS) for sample digestion and analyzed at the Isotopic Geology Laboratory (LGI-UFRGS) using high-resolution inductively coupled plasma mass spectrometry (HR-ICP-MS).



As a chemostratigraphic tool, proxies were generated to understand the recorded paleoenvironmental evolution. To evaluate the input of nutrients such as phosphorus into the system, excess phosphorus was calculated. Normalization is performed relative to the concentration of  $\text{Al}_2\text{O}_3$  in the sample and the average concentration of  $\text{Al}_2\text{O}_3$  in the continental crust (Schmitz et al., 1997). This process converts the mass percentage of phosphorus oxide to excess phosphorus, excluding the proportion of phosphorus related to minerals such as aluminosilicates in the system (eq. 1).

$$\text{eq.1} \quad P_{\text{ex}} = \frac{P_2O_5}{(\text{Al}_2O_3 * 0.15)}$$

To assess redox conditions, the following proxies were utilized. These proxies include elements whose behavior in a system changes with variations in environmental redox conditions. The stratigraphic investigation of these elements was conducted using the enrichment factor (EF), which indicates how enriched a sample is relative to average shale (AS) according to Wedepohl, (1971), as shown in equation (2).

$$\text{eq.2} \quad X_{\text{EF}} = \frac{(X_{\text{sample}}/A_{\text{sample}})}{(X_{\text{AS}}/A_{\text{AS}})}$$

The degree of pyritization (DOP<sub>T</sub>) is a simplified version of the DOP proxy; both estimate the amount of iron available in the system and retained in the form of sulfide (pyrite), thus characterizing the oxygenation level of the environment (Jones & Manning, 1994; Algeo, Thomas J. & Maynard, 2008) (eq.3).

$$\text{eq.3} \quad \text{DOP}_T = S_T * (55:85/64.12)/\text{Fe}_T$$

### 3.7 Organic carbon isotope

Organic carbon isotope analysis was conducted at the Lamir Institute of the Federal University of Paraná (UFPR). For sample preparation, 2 grams of each crushed sample were washed with HCl to remove carbonates and then cleaned five times with milli-Q water. The samples, placed in tin capsules, had their carbon converted to  $\text{CO}_2$  through dynamic combustion with oxygen injection at 1020°C. The

gaseous combustion products were purified and separated for subsequent analysis using the Thermo Scientific Delta V IRMS, where they were ionized and accelerated.

## 4. Results

### 4.1 Sedimentological characterization

#### 4.1.1 Facies analysis and facies associations

Based on the core descriptions, 11 facies were identified, as detailed in Table 1, including their lithology, structures, and interpretation. The facies associations were defined following (Burchette & Wright, 1992) for carbonate platforms. A summarized description of cores HV-54 and SC-15 is presented in Figure 2, along with the geophysical profiles.

Facies Code	Lithology	Sedimentary structure	Interpretation
Gmm	Matrix-supported, intraformational conglomerate, with clayey intraclasts up to 2 cm.	Massive; convolute bedding	Plastic, viscous debris flow with high internal cohesion; deformation by fluidization.
Sw/Fw	Very fine sandstone to siltstone, light grayish-yellow.	Low-angle truncated or cross-wavy lamination	Migration of subaqueous ripples under oscillatory flow.
Fm	Light gray siltstone to dark gray shale.	Massive or indistinct lamination. Locally irregular parting	Gravitational settling of suspended particles.
Fh	Silty to clayey shale, dark gray to black.	Plane-parallel lamination and millimetric to centimetric fissility. Locally, concentrations of pyrite and organic matter	Gravitational settling of suspended particles under reducing conditions.
Ht	Heterolithics composed of centimeter to millimeter-scale interbeds of very fine sandstone, siltstone, and claystone.	Heterolithic bedding (linsen, wavy, flaser), internally with truncated wavy lamination. Locally, it shows fissility	Variation between settling of suspended particles (clay) and migration of small-scale ripple forms under lower unidirectional or oscillatory flow regime.
Rt	Rhythmic intercalation (mm to cm scale) of cream-colored calcimudstone and dark gray shale.	Plane-parallel lamination.	Gravitational settling of suspended particles, with compositional variation between micrite and siliciclastic mud.

Br	Intraformational breccia supported by muddy matrix, light gray, with carbonate intraclasts up to 3-6 cm.	Carbonate intraclasts formed by 'teepees'; some fluidized clay films.	Plastic, viscous debris flow with high internal cohesion; deformation by fluidization, with mixture of intra- and extrabasinal constituents.
Mud(m)	Cream-colored calcimudstone.	Massive, locally with 'cone-in-cone' structure and irregular parting.	Gravitational settling of suspended carbonate mud.
Mud(w)	Cream-colored calcimudstone.	Wavy and/or low-angle cross lamination.	Gravitational settling of suspended carbonate mud, with slight bottom agitation by oscillatory flow.
Mud(h)	Cream-colored calcimudstone.	Plane-parallel lamination; fractured.	Gravitational settling with precipitation of carbonates and sediments.
Rdst	Rudstone with carbonate intraclasts up to 4 cm.	Horizontal lamination.	Subaerial exposure, drying, and reworking.

Table 1 Summarized description of observed facies and inferred processes.

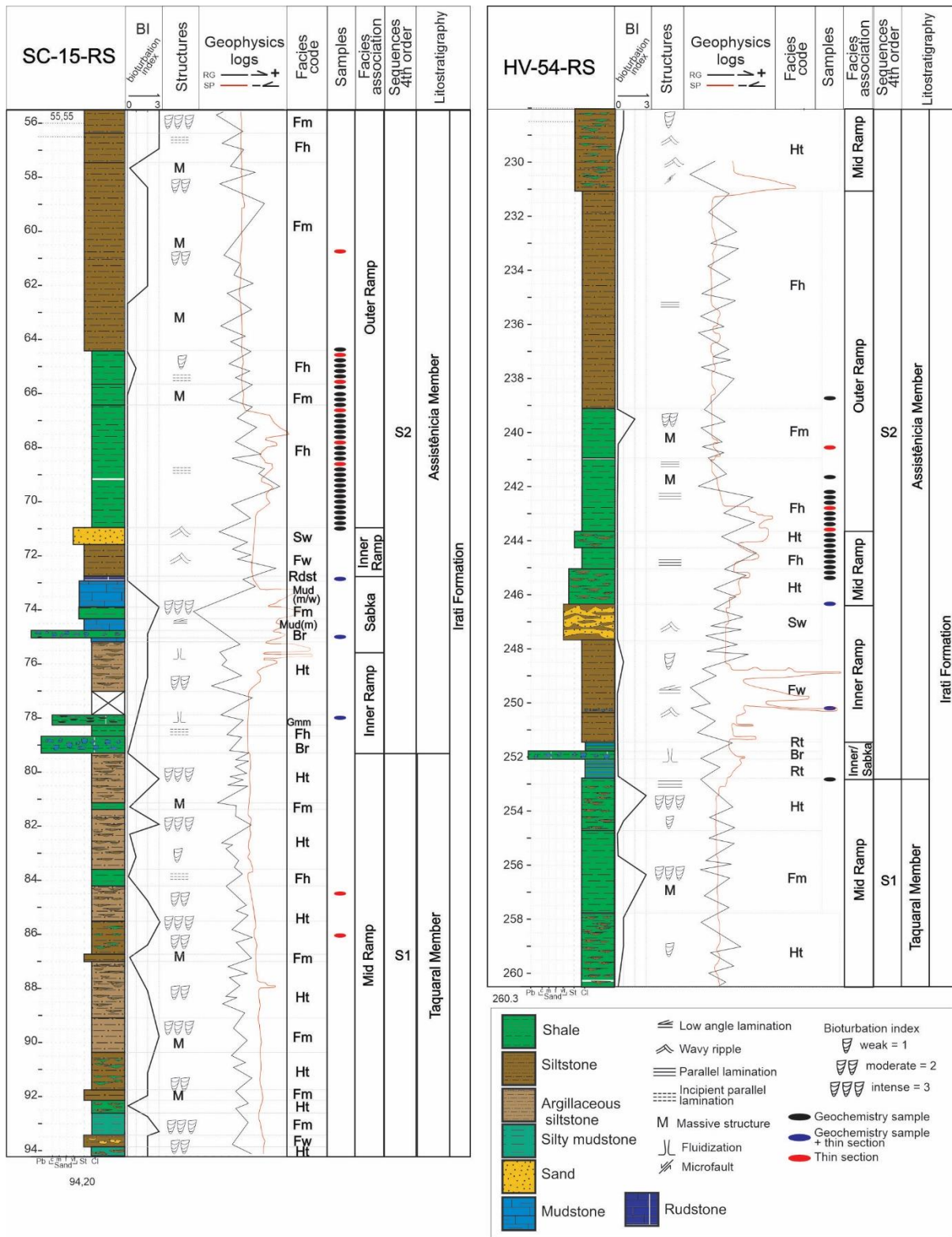


Fig. 2. Lithological logs with sample locations and the interpretation of facies associations. Lithostratigraphy and sequences according to Xavier et al 2018.

The identified facies associations in the cores are: outer ramp, intermediate ramp, inner ramp, and evaporitic coastal plain (sabkha). The Outer Ramp Facies

Association consists of muddy lithologies (lithofacies Fm and Fh – Fig. 4a-b), deposited through gravitational settling in low-energy environments (below the fair-weather wave base). The sedimentation is mixed, predominantly siliciclastic, with varying concentrations of organic matter. The abundance of pyrite in these lithologies indicates a predominantly reducing environment, likely due to the water depth (Fig. 4b). Bioturbation in this interval varies from none to intensely bioturbated.

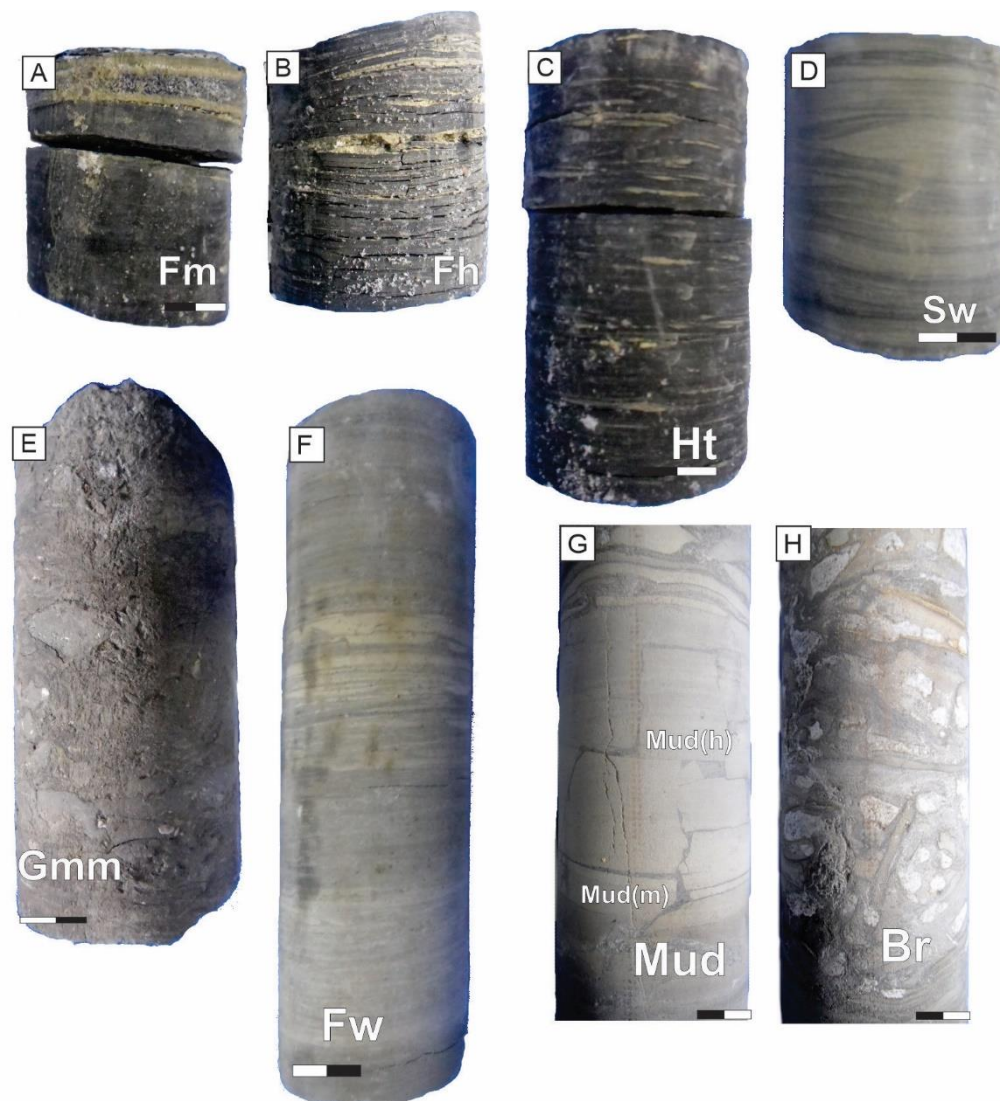


Fig. 3 - (A) Dark gray massive shale (Fm), (B) Dark gray parallel-laminated shale (Fh), (C) Heterolithic bedding (linsen) (Ht), (D) Very fine sandstone with wavy lamination (Sw), (E) Massive conglomerate (Gmm), (F) Light gray siltstone with low-angle lamination (Fw), (G) Massive (Mud(m)) and laminated (Mud(h)) calcimudstones, (H) Intraformational breccia with carbonate intraclasts (Br)

The Intermediate Ramp Facies Association includes lithologies deposited in a distal environment under wave action, between the fair-weather and storm wave base levels (lithofacies Ht, Fw, and Sw – Fig. 3c-d), as well as muddy lithologies deposited through gravitational settling under low-energy conditions (lithofacies Fm, Fh). The sedimentation is predominantly siliciclastic, with variations in organic matter concentration.

The Inner Ramp Facies Association includes intraclastic conglomerates and breccias resulting from wave reworking of semi-consolidated carbonate and muddy sediments (lithofacies Gmm and Br – Fig. 3e) and heterolithic and fine-grained lithologies deposited under wave action (lithofacies Ht, Fw, and Sw – Fig. 3f). This association represents predominantly siliciclastic sediments deposited above the fair-weather wave base. The Sabkha Facies Association is composed of calcareous rudstones and calcimudstones (Rt, Rdst, Mud(m), Mud(w), and Mud(h) – Fig. 3g-h).

The SC-15 well displays a complete regressive-transgressive cycle, with the Intermediate Ramp Facies Association (FA) at the base, transitioning to the Inner Ramp FA and Sabkha FA during the maximum regression interval, including 'teepees.' From the middle to the top, the well records Inner Ramp and Outer Ramp FAs (Fig. 2). In contrast, the HV-54 well begins with the Intermediate Ramp FA at the base, transitions to the Inner Ramp FA and Sabkha FA in the central portion, and finally culminates with an intercalation of Outer and Intermediate Ramp FAs at the top (Fig. 2).

#### **4.1.2 Stratigraphic framework**

Based on databases provided by the Geological Survey of Brazil (SGB) and previous studies conducted in the southern portion of the basin, it was possible to define and correlate the specific interval for geochemical sample collection in the Irati Formation. This positioning was based on studies by Araújo (2001), Xavier et al. (2018), Bastos et al. (2021), and Cagliari et al. (2022), conducted in the same sampling region as this study. Regarding the stratigraphic positioning, the interval spans from the Taquaral Member to the middle portion of the Assistência Member, using carbonate levels as reference points. The detailed chemostratigraphy sampling is specifically positioned in the lower black shale of the Assistência Member, located immediately after the first carbonate level.

### 4.1.3 Compositional analysis

Among the 16 thin sections analyzed, 11 are mudstones associated with the Outer Ramp and Intermediate Ramp facies associations. Three sections consist of a very fine sandstone, a conglomeratic sandstone, and a mudstone from the Inner Ramp facies association. Additionally, two sections are carbonate crusts from the Sabkha facies association. The quantification of the matrix, along with extrabasinal, intrabasinal, and diagenetic constituents, was organized by facies association and presented in individual bar charts for each thin section (Fig. 4).

The mudstones from the Outer Ramp FA typically contain a higher average amount of matrix, around 68% (Fig. 4 and 5-a). Significant differences in average matrix content are observed between the SC-15 and HV-54 wells. SC-15 core shows a greater proportion of siliciclastic matrix rich in organic matter compared to HV-54, especially in the samples 60.7 m and 64.6 m deep.

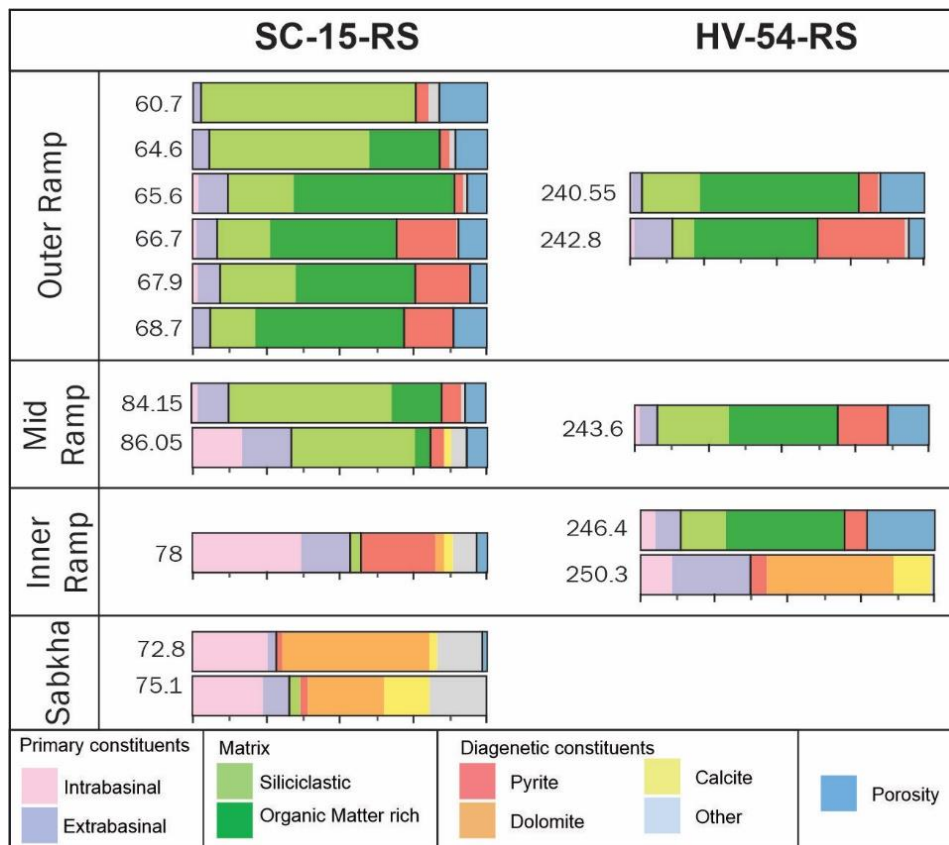


Fig. 4 – Quantification of primary constituents, matrix, diagenetic constituents, and porosity based on petrographic descriptions, grouped by well and Facies Association.

Extrabasinal constituents average 6.83% in both wells, primarily composed of quartz (average 3.37%, with a maximum of 4.33%), muscovite (1.5%), and amorphous organic matter (average 1%), with lesser amounts of biotite, celadonite, and zircon. Intrabasinal constituents are less than 1% in both wells, with sporadic occurrences of spores, clay pellets, and phosphatic bioclasts. Diagenetic constituents average 14.04%, with pyrite being prominent in framboidal and/or microcrystalline forms (Fig. 5-b), averaging 18% (with a maximum of 29%) in the HV-54 core and 11% (with a maximum of 20.3%) in the SC-15 core. Additionally, gypsum fills fractures, and lamellar kaolinite replaces muscovite, with the latter observed only in the SC-15 core. Porosity in both wells is approximately 10%, predominantly in fractures.

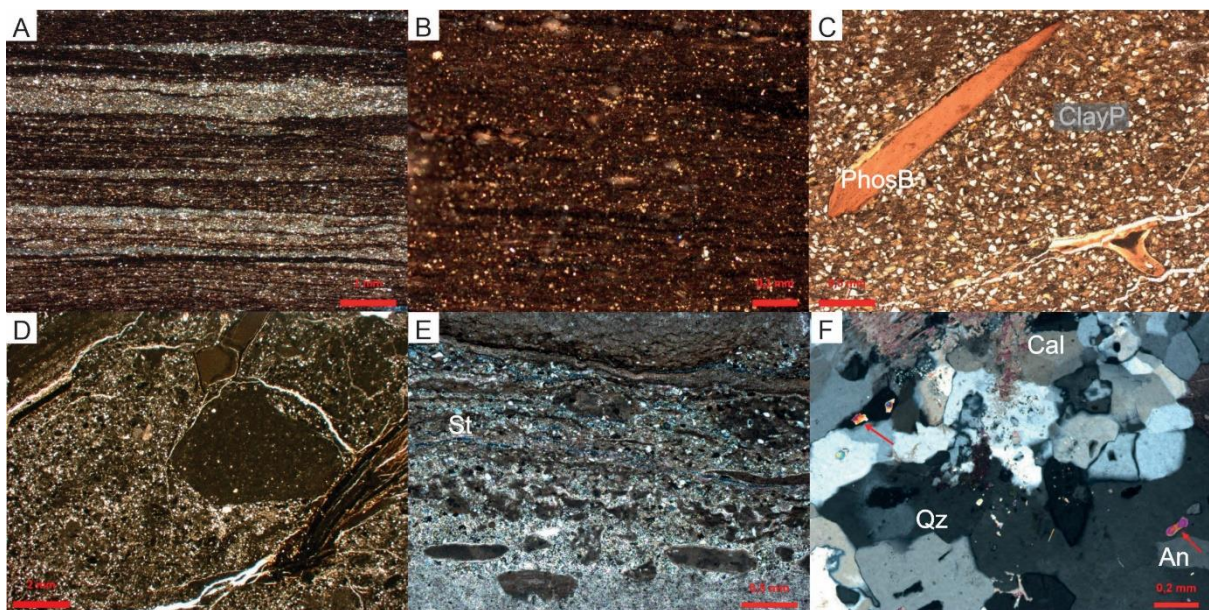


Fig. 5 – Photomicrographs of a (A) laminated silty shale with a matrix rich in amorphous organic matter. (B) Framboidal pyrite replacing a clay-rich matrix with abundant organic matter. (C) Phosphatic bioclasts (PhosB) and clayey peloids (clayP). (D) Hybrid conglomerate, fractured, rich in intraclasts and carbonate and clayey peloids. (E) Carbonate crust with stylolites, peloids, and carbonate intraclasts. (F) Chalcedony and mega-quartz (Qz) replacing anhydrite nodules (An) and macrocrystalline calcite (Cal) filling pores.

The samples from the Inner Ramp display varied lithologies, including a mudstone (sample at 246.4 m), a very fine sandstone (sample at 250.3 m), and a conglomeratic sandstone (sample at 78 m). The mudstone is similar to those described in other facies associations, characterized by a predominance of organic-rich matrix (40.33%), with extrabasinal constituents (8.66%) exceeding intrabasinal constituents (5%), and pyrite as the primary diagenetic constituent (7.66%). The very fine sandstone has a



primary composition largely made up of extrabasinal constituents, predominantly quartz (19%) and feldspars (3.5%), with no matrix. Its diagenetic composition is primarily dolomite (44%) and calcite (12%). The conglomeratic sandstone is composed mostly of intrabasinal constituents, including notable amounts of peloids (13%) and carbonate intraclasts (10%). Pyrite (25%) is the main diagenetic constituent, occurring mainly in a microcrystalline habit. Additionally, chalcedony and quartz are present, replacing anhydrite.

The samples from the sabkha FA consist of carbonate crusts, which contain up to 90% carbonate. These crusts are made up of carbonate intraclasts, and carbonate peloids. They have a maximum of 3.67% siliciclastic matrix and no organic matter. Extrabasinal constituents (6%) include quartz (3.83%), muscovite (0.83%), biotite (0.5%), and plagioclase (0.5%). Intrabasinal constituents (24.5%) are mainly carbonate intraclasts (19.3%), phosphatic bioclasts, clay and carbonate peloids. Diagenetic products account for 66.65% and include primarily dolomite (37.98%). Dolomite occurs as a continuous rim covering primary constituents or in blocky, macrocrystalline forms, replacing matrix and grains, as microcrystalline crusts replacing matrix, as intragranular dolomite in undifferentiated grains and peloids, and in saddle shapes filling fractures or replacing barite in fractures. Additionally, poikilotopic and macrocrystalline calcite (9%), chalcedony (5.34%), as well as quartz, dickite, barite, and chalcedony are present. Fracture porosity averages less than 1%.

## **4.2 Geochemistry composition**

### **4.1. Total organic carbon and sulfur contents**

The stratigraphic assessment of Total Organic Carbon (TOC) and sulfur (S) allowed for the identification of five intervals, each characterized by specific behaviors of these parameters. These intervals are: 'Pre-Organic', 'Organic Increment', 'Organic Stability 1 and 2', and 'Low Organic', all of which were identified in the SC-15 well. The 'Pre-Organic' interval is marked by a nearly stable behavior of TOC and S, with averages of 3.34% and 1.61%, respectively. The 'Organic Increment' interval is characterized by a gradual increase in TOC, starting at 3.59% and reaching 10.60%. During this interval, sulfur (S) shows a negative correlation with TOC. In the 'Organic Stability' intervals, TOC and sulfur concentrations fluctuate around averages of 12.95% for TOC and 1.09% for sulfur. Between the stability interval and the 'Low Organic' interval, a sharp decline in TOC values

(from 12.70% to 2.99%) and sulfur values (from 1.18% to 0.28%) is observed in the SC-15 well. In the final 'Low Organic' interval, both TOC and sulfur values remain low and stable, at 1.24% and 0.11%, respectively. Due to its distance from the other samples, the sample at 60.70 meters will not be considered in the description of geochemical trends.

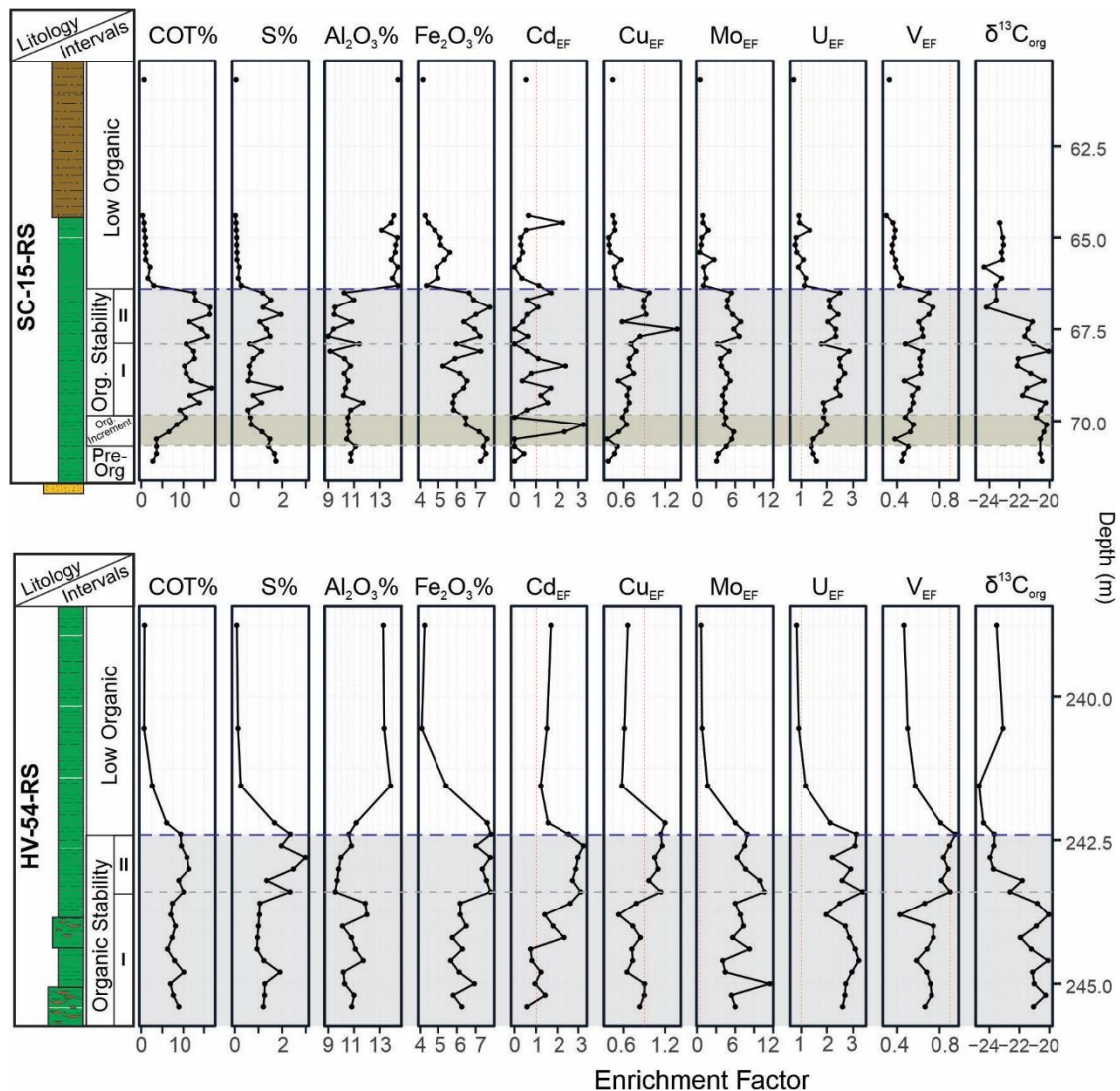


Fig. 6. Stratigraphic Distribution of TOC, S, and Major Oxides ( $\text{Al}_2\text{O}_3$  and  $\text{Fe}_2\text{O}_3$ ). Enrichment Factor of Redox-Sensitive Elements (Cd, Cu, Mo, U, and V) and Organic Carbon Isotope.

In the HV-54 well, only the 'Organic Stability' and 'Low Organic' intervals were identified. During the 'Organic Stability 1' interval, TOC fluctuates around an average of 8.43%. In the 'Organic Stability 2' interval, sulfur exhibits erratic behavior, with some samples showing high sulfur concentrations (a maximum of 2.98% in the sample at depth 244.4 meters). The transition to the 'Low Organic' interval is less abrupt in this well

compared to SC-15. Despite the limited number of samples in this interval, there is relative stability in the parameters, with low TOC and sulfur values averaging 1.64% and 0.2%, respectively.

## 4.2. Major elements

In the ternary plot of  $\text{SiO}_2$ ,  $\text{Al}_2\text{O}_3$ , and  $\text{CaO}$ , samples from both wells show enrichment in silica, with average values of 49.12%  $\text{SiO}_2$ , 11.39%  $\text{Al}_2\text{O}_3$ , and 0.76%  $\text{CaO}$ . No significant differences were observed between the samples from the two cores or between intervals. Stratigraphically, major elements exhibit distinct behaviors in both wells (Fig. 6). In SC-15, the major oxides show a stable trend until the TOC shift, where a sudden change to higher concentrations occurs. In contrast, in HV-54, the change in behavior occurs gradually during the Low Organic interval.

Generally, all oxides follow a similar pattern to  $\text{Al}_2\text{O}_3$ , except for  $\text{Fe}_2\text{O}_3$  concentration. In the SC-15 well,  $\text{Fe}_2\text{O}_3$  shows a negative trend until the Stability 1 interval, whereas in the HV-54 well, it maintains a stable pattern in the same interval.  $\text{Fe}_2\text{O}_3$  concentrations are high and stable in both cores during the Stability 2 interval, with an abrupt negative shift in SC-15 and a gradual decrease in HV-54 during the Low Organic interval.

## 4.3 Redox-sensitive elements

The vertical distribution of redox-sensitive elements in Figure 6 displays a red dashed line at  $\text{EF}=1$ , representing the average shale. Values above this line are considered enriched in the element relative to AS, while values below 1 indicate that the element is depleted compared to AS.

The enrichment factor (EF) of cadmium (Cd) in the SC-15 well is the most erratic among the redox-sensitive elements. However, it is noticeable that the average line in the Pre-Organic interval (0.5) is lower than the values observed in the Organic Increment interval, which shows a positive trend reaching values above 3. The Organic Stability interval for redox-sensitive elements can also be subdivided into Stability Interval 1 and Stability Interval 2. In Stability Interval 1, extending to the sample at 67.90 meters, the EF of Cd lacks a defined pattern but maintains an intermediate baseline between 0 and 2.5,

not reaching the values seen in the Organic Increment interval. In Stability Interval 2, the EF of Cd shows a positive trend up to approximately 1.75. During the Low Organic interval, the EF of Cd follows the negative shift in TOC and returns to a low baseline near 0.5, similar to the Pre-Organic interval.

Copper (Cu) and vanadium (V) exhibit a positive trend from the Pre-Organic interval up to the top of the Organic Stability 1 interval. After this, both elements stabilize, with average enrichment factors of 0.9 for  $Cu_{EF}$  and 0.6 for  $V_{EF}$ . In the Low Organic interval, a negative shift in the enrichment factors of these elements is observed, with stability at lower values, with  $Cu_{EF}$  around 0.45 and  $V_{EF}$  around 0.4. The enrichment factors of molybdenum ( $Mo_{EF}$ ) and uranium ( $U_{EF}$ ) show similar behaviors. Both start with values above the average shale (AS) enrichment.  $Mo_{EF}$  exhibits a positive trend in the Pre-Organic and Organic Increment intervals, stabilizing at an average of 4.5 in Stability Interval 1. At the base of Stability Interval 2,  $Mo_{EF}$  shows a positive increment followed by a negative trend. The behavior of  $Mo_{EF}$  aligns with the negative shift in TOC, stabilizing near the AS baseline in the Low Organic interval with values around 1.5.  $U_{EF}$ , on the other hand, shows a negative trend in the Pre-Organic interval, switches to a positive trend during the Organic Increment and Stability 1 intervals, reaching a maximum value of 2.75. Like  $Mo_{EF}$ ,  $U_{EF}$  also changes behavior at the base of Stability Interval 2. However, for uranium, the negative shift in EF is followed by a stability trend with values lower than those in the previous interval, averaging around 2.25. The Low TOC interval begins with a negative shift and stabilizes with a trend close to the average shale line.

In the HV-54 well, the behavior of Cd enrichment factor ( $Cd_{EF}$ ) is more consistent compared to SC-15. In Stability Interval 1,  $Cd_{EF}$  shows a positive trend, indicating Cd enrichment relative to the average shale (AS). In Stability Interval 2, it maintains a baseline around 3, which decreases to close to 1 (AS) in the Low Organic interval. Similarly to the SC-15 well, the enrichment factors for copper (Cu) and vanadium (V) in HV-54 also exhibit comparable patterns. Both elements remain stable and depleted relative to AS in Stability Interval 1, with  $Cu_{EF}$  around 0.75 and  $V_{EF}$  around 0.65. In Stability Interval 2, the enrichment factors for these elements show a positive shift, stabilizing near a baseline close to 1 (AS). As TOC values decrease,  $Cu_{EF}$  and  $V_{EF}$  exhibit a negative trend until they stabilize in the low Organic interval, with  $Cu_{EF}$  at 0.6 and  $V_{EF}$  at 0.5. Similarly to the SC-15 well, the enrichment factors for molybdenum ( $Mo_{EF}$ ) and uranium ( $U_{EF}$ ) in HV-54 start with values indicating enrichment above the average shale (AS).  $Mo_{EF}$  exhibits a stable trend at 6.20 in

Stability Interval 1. After a positive shift at the base of Stability Interval 2, it maintains a positive trend until the Low Organic interval, where it stabilizes close to the average shale. The enrichment factor for uranium ( $U_{EF}$ ) maintains a baseline of 2.75 until the end of Stability Interval 2, after which it starts a negative trend and stabilizes near 1 in the Low Organic interval.

#### **4.5 Organic Carbon Isotope**

The organic carbon isotope signature ( $\delta^{13}C_{org}$ ) was assessed based on the stratigraphic positioning of the samples as shown in Figure 6. Organic carbon isotope values range from -24.35‰ to -20.05‰ in the SC-15 well and from -24.68‰ to -20.04‰ in the HV-54 well. Both cores exhibit similar behavior. They start with a positive trend in the isotope signature up to the top of the Organic Stability Interval 1. In Organic Stability Interval 2, they show a negative trend until the TOC shift and then stabilize at more negative values in the Low Organic interval.

### **5 Discussion**

#### **5.1 Sedimentology**

The facies succession described in the two wells agrees with the interpretation that the deposition of the Irati Formation occurred in a carbonate ramp environment (Araújo, 2001; Xavier et al., 2018). The predominance of proximal facies in the SC-15 well, compared to HV-54, suggests a possible reduction in water depth towards the location of this well. In addition to the well-developed heterolithic facies, SC-15 also exhibits a higher percentage of carbonate facies in the inner ramp and sabkha facies associations. The presence of anhydrite and chalcedony nodules in samples from 78.00 m and 75.10 m of this core indicates a dry and warm environment, characterizing the evaporitic nature of this interval. The shallow-water conditions, and evaporitic environmental are common in Irati Formation, particularly in the northern portion of the basin where these facies are more abundant (Hachiro, 1997; Araújo, 2001; Antunes et al., 2022; Petri et al., 2022).

The differentiation between the two wells is also evident from the quantitative analysis of petrographic constituents, which reveals a relative enrichment of fine-grained constituents in HV-54, accompanied by a higher proportion of organic-rich matrix. This supports the idea that the HV-54 well is closer to the depocenter, compared to the SC-15

core. Grain size and selection are important sedimentological conditions for the preservation of organic matter. Therefore, distal, lower-energy environment where fine materials such as clay and silt are deposited not only favors organic matter deposition but also provides more reducing conditions for its preservation. Previous studies before 2000 suggested that the geological structure of southern Rio Grande do Sul was a high topographic feature that acted as a barrier to the circulation of the Irati-Whitehill Sea further inland, towards what is now the American continent. Araújo (2001), however, indicates that this morphological structure was submerged at that time. Nonetheless, our data suggest that, even when submerged, this feature still functioned as a local paleorelief, indicating a variation in paleobathymetry, with the basin deepening towards the west.

## **5.2 Paleoenvironmental Proxies**

### **5.2.1 Detrital Input**

To evaluate the detrital contribution during the deposition of the lower organic-rich shales in the Irati Formation, stratigraphic distributions of aluminum concentration in mass percent, and the silicon-to-aluminum (Si/Al) and titanium-to-aluminum (Ti/Al) ratios were used (Fig. 8, red curves) (Sageman & Lyons, 2003).

In the SC-15 well, only the aluminum concentration (Al%) and the silicon-to-aluminum ratio (Si/Al) showed changes in behavior corresponding to the Organic intervals, while the titanium-to-aluminum ratio (Ti/Al) remained stable across all intervals. The behavior of aluminum concentration (Al), an indicator of aluminosilicate minerals such as clays, is stable and low, with an average of 5.5% from the “Pre-Organic” interval to the “Organic Stability 2” interval. This indicates a steady supply of minerals from this group. The start of the Low Organic interval is marked by a shift in the system leading to stabilization of Al at a higher average concentration (7.5%). The indicator of silicates such as quartz, also used as a proxy for grain size, shows a negative trend until the Low Organic interval, without any abrupt behavioral changes. This suggests a gradual decrease in the input of these minerals and/or a consecutive reduction in grain size.

In the HV-54 well, all detrital input proxies show patterns associated with organic matter accumulation (TOC). During the Organic Stability 1 interval, the Al% indicates a stable contribution of aluminosilicates. At the beginning of the Organic Stability 2 interval, this contribution decreases but then follows a positive trend, stabilizing in the Low Organic

interval with a high input of these minerals (7%). The Ti/Al ratio, used to detect the input of heavy minerals like titanite and rutile, shows a trend of decreasing heavy mineral concentration until the beginning of the Organic Stability 2 interval, after which it returns to average concentrations of heavy minerals (5.5%) and stabilizes until the Low Organic interval.

The Si/Al ratio displays two disconnected negative trends: one in the Organic Stability 1 interval and another starting in the Organic Stability 2 interval and continuing to the second sample of the Low Organic interval. These data suggest two main detrital inputs into the system, marked by the two positive peaks in Si/Al and Ti/Al. It can also be inferred that the first detrital input is enriched in heavy minerals compared to the second. Although indicated by other proxies, these two inputs do not significantly alter the TOC but are marked by a peak in sulfur percentage (S%) that delineates the boundary between the Organic Stability 1 and 2 intervals.

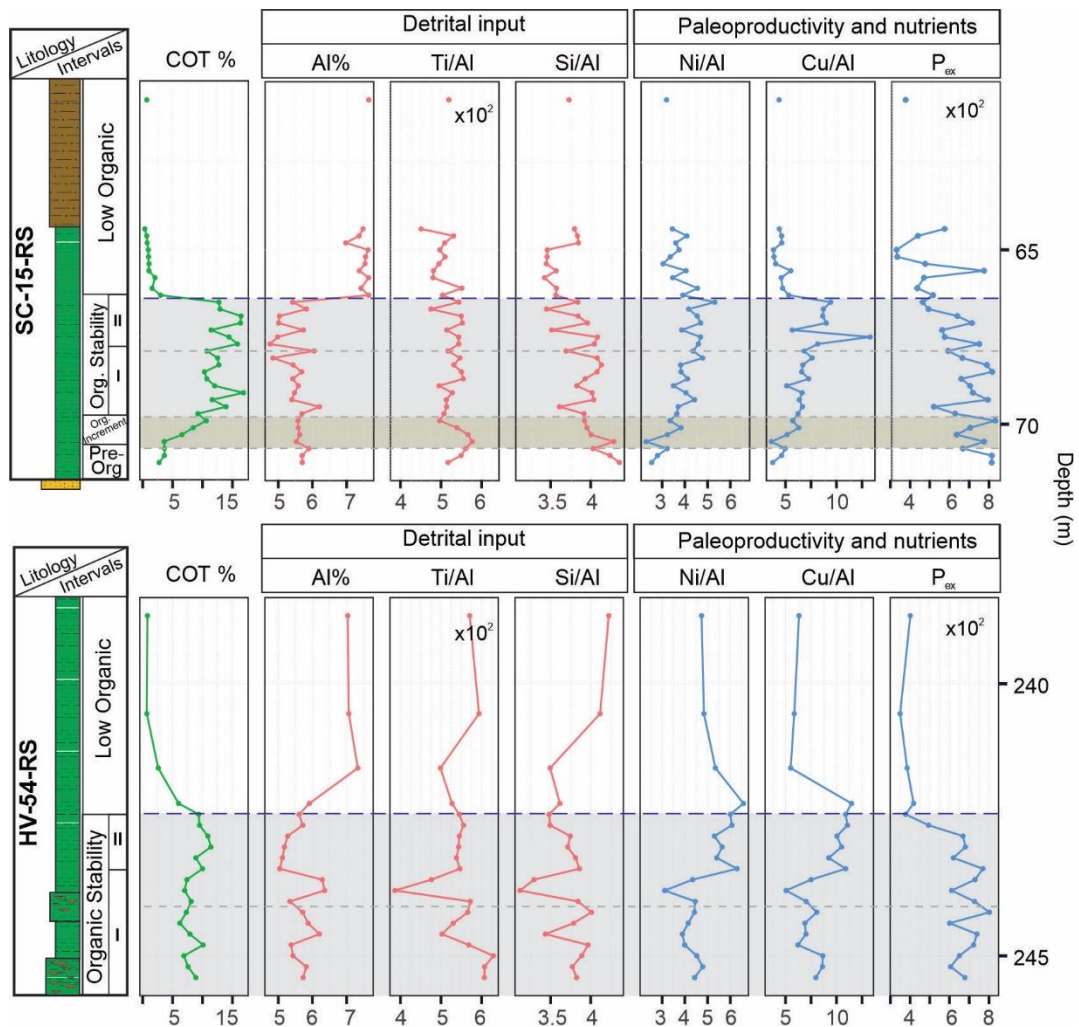


Fig. 7. Stratigraphic Distribution of TOC, Detrital Proxies (Al%, Ti/Al, and Si/Al), and Proxies of Primary Productivity and Nutrients (Ni/Al, Cu/Al, and P<sub>ex</sub>)

### 5.2.2 Nutrients and Paleoproductivity

The stratigraphic behavior of the Nickel/Aluminum (Ni/Al) and Copper/Aluminum (Cu/Al) ratios, as well as the phosphorus excess (P<sub>ex</sub>) for the two cores, is presented in Figure 7. Nickel (Ni) and copper (Cu) are commonly deposited as organometallic complexes associated with organic matter (OM) (Tribovillard, 2021). High paleoproductivity increases OM deposition, which favors the preservation of these metals. In anoxic and euxinic environments, anaerobic bacteria release hydrogen sulfide (H<sub>2</sub>S) during the decomposition of OM, which can react with the complexed metals, leading to the formation of sulfides such as pyrite.

Phosphorus (P) is generally an important nutrient for photosynthetic organisms. During periods of high primary productivity, biomass production also increases, leaving



phosphorus anomalies recorded in the sediment (Schmitz et al., 1997; Percival et al., 2020).

In the SC-15 well, the Ni/Al ratio exhibits two trends: an initial positive trend up to the top of the Stability 1 interval, followed by a negative trend through the Low Organic interval. The Cu/Al ratio also shows a positive trend up to the top of the Stability 1 interval but then exhibits irregular behavior, with a higher average value at the end of the previous interval. The Low Organic interval is marked by an abrupt change in the system, leading to stabilization at a lower average value. Excess phosphorus shows a single negative trend extending to the Low Organic interval. In this core, both Ni/Al and Cu/Al indicate higher values associated with high Organic intervals, suggesting a correlation with increased productivity.

In the HV-54 well, the Ni/Al and Cu/Al proxies display similar behavior. Both are stable at a medium baseline level during the Organic Stability 1 interval. A possible indication of increased paleoproductivity is observed when both proxies show a positive shift and stabilize at a higher baseline level compared to Stability 1, continuing into the Low Organic interval. However, phosphorus excess demonstrates stable behavior with a high average value that persists into the Low Organic interval.

### **5.2.3 Redox Conditions**

To evaluate the redox conditions of the water column, proxies such as DO<sub>Pt</sub>, Fe/Al, V/Cr, Ni/Co, and V/(Ni+V) were assessed. The V/Cr, Ni/Co, and V/(Ni+V) ratios assess redox conditions based on the specific behavior of trace elements. Vanadium and nickel are complexed with organic matter, while chromium and cobalt are associated with detrital input (Hatch & Leventhal, 1992; Jones & Manning, 1994). The Fe/Al ratio evaluates the enrichment of iron in the system by dividing the total iron concentration by the aluminum concentration in the sample, which normalizes the iron concentration relative to aluminosilicates (Lyons & Severmann, 2006).

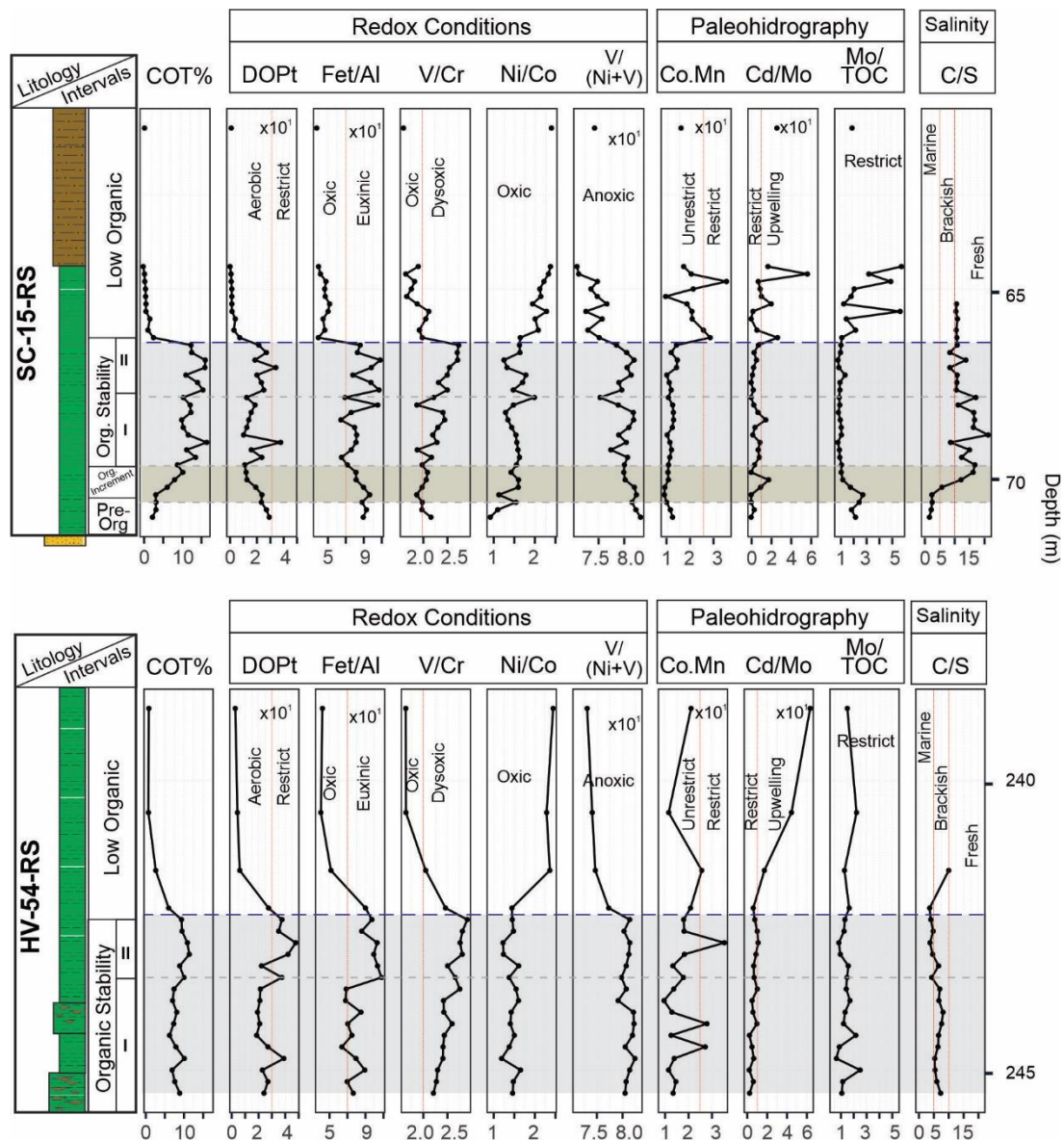


Fig. 8. Stratigraphic Distribution of TOC, Redox Proxies (DOPt, Fet/Al, V/Cr, Ni/Co and V/ V+Ni), Paleohydrography proxies (Co\*Mn, Cd/TOC and Mo/TOC) and Salinity proxies (C/S)

The DOPt values for samples from both wells indicate that the sediments were predominantly deposited under aerobic conditions, which limits pyrite formation. The oxidative condition is also assessed by the Ni/Co ratio. However, the analyzed samples show consistently low and constant sulfur content, regardless of iron concentration. This may indicate a sulfur deficiency in the environment, typically associated with low sulfate concentrations, characteristic of non-marine waters. It is also important to note that DOPt is a simplification based on the stoichiometry of pyrite, assuming that all the sulfur in the sample corresponds to the sulfur in pyrite. However, in samples rich in organic matter, some of the sulfur is also associated with the organic matter, which can complicate the

interpretation of this proxy.

The oxic scenario is not reflected in the assessment of other proxies, which indicate that some intervals experienced more reducing conditions. For instance, the  $V/(Ni+V)$  ratio suggests that all samples were deposited in an anoxic environment, with intervals close to the euxinic threshold. This is corroborated by the  $Fe_t/Al$  proxy, which shows that samples were deposited under euxinic conditions, though those from the stability interval 2 exhibit even higher iron enrichment. This same proxy indicates oxic conditions for samples from the low Organic interval. Additionally, the  $V/Cr$  proxy groups samples from the pre-Organic and Organic increment intervals (SC-15) along with samples from the low Organic interval, all deposited in an oxic environment. Meanwhile, other samples fall within a dysoxic environment range.

The ternary diagram TOC-Fe-TS (Fig. 9) is suggested as an alternative to approximate the degree of pyritization (Arthur & Sageman, 1994). In this diagram, samples from the stability intervals of both wells are grouped in a dysoxic trend, with an approximate pyritization degree of 0.56. Samples from the low Organic interval are situated in a trend with higher Fe and lower S and TOC, indicating a pyritization degree of less than 0.1. Additionally, samples from the pre-Organic interval and one from the Organic increment interval fall into the oxic field.

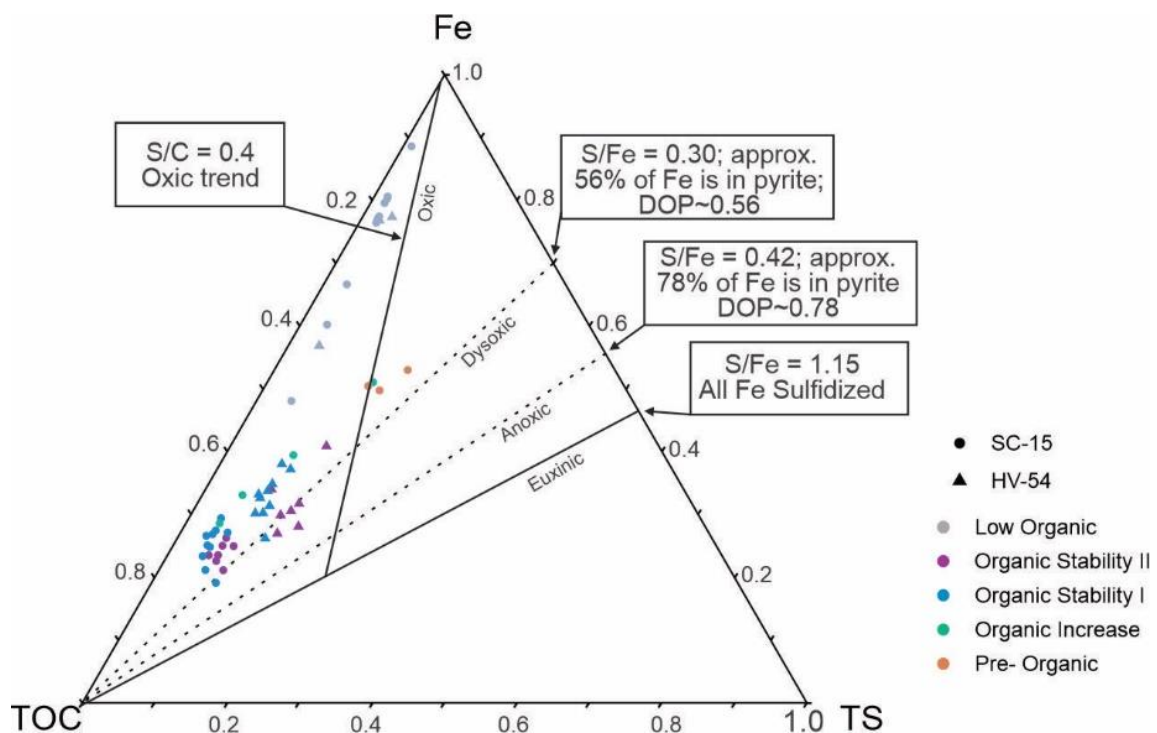


Fig. 9. Ternary plot of TOC-Fe-TS with stability fields (Modified from Arthur and Sageman, 1994)

#### 5.2.4 Paleohydrography and Salinity

The proxies used to characterize the paleohydrography of the studied interval were Co\*Mn, Cd/Mo, and Mo/TOC. The Mo/TOC and Cd/Mo suggests that all samples were deposited in a highly restricted environment (Mo/TOC <15, and Cd/Mo<0.1) (Algeo, Thomas J. & Lyons, 2006; Sweere et al., 2016). In contrast, the stratigraphic behavior of the and Co\*Mn proxies indicates deposition in a non-restricted environment and/or one influenced by upwelling (Sweere et al., 2016; McArthur, J. M., 2019). Salinity, evaluated using the C/S ratio (carbon-total organic carbon and sulfur), shows variation in salinity between the two wells (Berner & Raiswell, 1984; Wei & Algeo, 2020). In core SC-15, the pre-Organic interval has marine salinity conditions that evolve into a freshwater condition during Organic Stability intervals 1 and 2, before shifting to a brackish condition in the low Organic interval. However, HV-54 remains under brackish condition. This technique, which is exclusively used for samples with TOC greater than 1, prevents distinguishing between marine and brackish environments. Wei & Algeo, (2020) suggest using the Sr/Ba and Ga/B proxies as alternatives for more accurate paleosalinity determination.

### 5.3 Paleoenvironmental Model

Based on the integration of facies and petrographic descriptions with detailed geochemistry, the richest interval of organic matter within the Irati Formation was characterized. This integration allowed the reconstruction of the paleoenvironmental history of this deposition and the identification of potential triggers for the significant accumulation and preservation of organic matter (OM). In this context, it was possible to infer a paleobathymetric positioning of the cores within the basin based on the facies associations found. In core SC-15, located to the east, there is a greater development of proximal facies, with the presence of carbonates and evidence of subaerial exposure. In contrast, core HV-54, situated to the west, predominantly exhibits lithologies indicative of a more distal environment. Araújo, (2001) notes that the southern Rio Grande do Sul shield was submerged during the deposition of the Irati Formation. However, our data suggest that, even while submerged, this feature acted as a paleorelief, indicating a local paleobathymetry with deepening of the basin towards the west. This configuration is

confirmed by the chemostratigraphic behavior, which reveals differing evolutionary patterns of anoxia in the two cores.

In SC-15, the studied shale is preceded by a package of fine-grained sandstones with wavy ripples. Two chemostratigraphic intervals occur before the organic enrichment: the pre-organic interval, characterized by TOC levels lower than 5%, and the interval of organic increment, which shows a gradual evolution of the system, by an increase in TOC but also by higher primary productivity proxies (Ni/Al and Cu/Al) and salinity proxies (C/S), alongside a reduction in detrital input parameters such as Si/Al and Ti/Al. In HV-54, the studied interval begins with heterolithic facies with already high TOC, leading to the organic-rich shales. Thus, the TOC behavior appears to reflect the positioning of these cores: in the deeper-water HV-54, characterized by more distal facies, no significant geochemical transition was recorded. These two intervals are possibly absent in HV-54 because it was already in a deeper and more stable condition at the onset of the enrichment process. In contrast, the shallower-water, more proximal deposits in SC-15 show a gradual increase in TOC. The behavior of detrital proxies mainly reflects the facies of which each sample. In SC-15, where the geochemical study interval consists solely of shales, the proxies show consistent trends until organic enrichment. In HV-54, the first interval is marked by erratic behavior in various proxies, consistent with heterolithic facies.

During the Organic Stability intervals, organic carbon remains high (>10% in core SC-15 and between 5% and 10% in core HV-54). These intervals are characterized by a low input of aluminosilicates and other detrital minerals, as evidenced by the Al%, Si/Al, and Ti/Al ratios. Conversely, the increases in Cu/Al, Ni/Al, and Pex suggest elevated productivity during these periods. This pattern of enrichment in productivity proxies in the HV-54 core was restricted to Organic Stability Interval 2, as Organic Stability Interval 1 showed erratic behavior due to lithology. In the SC-15 core, Stability Intervals 1 and 2 are characterized by consistently low salinity, whereas the HV-54 core maintained indicators of brackish water. This less saline interval correlates with peaks of primary productivity is also reported through organic biomarkers in studies conducted near the study area (Bastos et al., 2021) and in the central part of the basin in the region of São Mateus do Sul in Parana State (Martins, Laercio Lopes et al., 2020; Martins, Laercio L. et al., 2021; Nascimento et al., 2021). Additionally, this interval coincides with a positive excursion in  $\delta^{13}\text{C}_{\text{org}}$ , possibly indicating a reduction in isotopic difference between organisms and  $\text{CO}_2$  due to  $\text{CO}_2$  depletion caused by increased primary productivity, supporting previous studies (Rau et al.,

1992; Oehlert & Swart, 2014).

The redox-sensitive elements molybdenum and uranium show enrichment within the organic stability intervals, while cadmium, cobalt, and copper only demonstrate enrichment in Organic Stability Interval 2 of the HV-54 core. The proxies indicating redox conditions, such as  $Fe/Al$  e  $V/(Ni+V)$ , vão de acordo com os elementos sensíveis as condições redox e indicam um ambiente pouco a não oxigenado variando de anoxico a euxinico. In contrast, the DO<sub>Pt</sub> indicators suggest oxic conditions for the deposition of the organic stability interval. The low DO<sub>Pt</sub> might be associated with low dissolved sulfate concentrations, as total sulfur is used in this proxy (Capone & Kiene, 1988; Segarra et al., 2013). The  $Ni/Co$  and  $V/Cr$  proxies also show inconsistencies with  $Fe/Al$  data and the enrichment of elements sensitive to redox conditions. According to Algeo, this behavior of bimetallic proxies discourages their use compared to enrichment proxies or those involving Fe.

Similarly, the paleohydrographic indicators do not point to a single condition. While the  $Mo/TOC$  and  $Cd/Mo$  proxies indicate a restricted environment for the deposition of shales in this interval, the  $Co^*Mn$  proxy suggests a non-restricted and/or upwelling environment. Nonetheless, the combined assessment of the hydrographic restriction proxies  $Co^*Mn$  and  $Cd/Mo$  helps distinguish the conditions that favored the high concentrations of organic matter in the Organic stability interval. Cadmium (Cd) is related to paleoproductivity due to its association with the metabolism of phytoplankton (Bruland, 1980; Sunda, 2012). This integrated approach provides a deeper understanding of the factors influencing the deposition and preservation of organic matter in marine environments, revealing the complex interactions between hydrographic dynamics and primary productivity.

In the graph shown in Figure 10, samples from the organic stability interval lie within the upwelling field, characterized by low  $Co^*Mn$  values. These samples group alongside those from the Cariaco Basin, which, like the Black Sea, is a restricted environment. In this context, intermediate  $Cd/Mo$  values suggest intense primary productivity, indicating a hybrid basin behavior that combines hydrographic restriction with intermittent upwelling. (Sweere et al., 2016). Algeo describes this behavior of occasional upwellings as reflecting temporal redox variations of low frequency.

The similar behavior of organic matter-rich samples in this study with those from the Cariaco Basin helps elucidate the depositional environment of the lower shale in the

Irati Formation. In the Cariaco Basin, the upwelling of deep waters triggers an increase in productivity, while the Irati-Whitehill Sea experiences a similar boost driven by the influx of freshwater. This freshwater influx, along with the subsequent reduction in salinity, is correlated with an increase in bacterial activity (Martins, Laercio Lopes et al., 2020; Bastos et al., 2021; Martins, Laercio L. et al., 2021; Nascimento et al., 2021; Brito et al., 2024). However, the source of this freshwater input is not fully understood. If it were associated with fluvial input, it would not have contributed minerals, as no significant changes are observed in detrital input proxies. A second hypothesis is a change in halocline conditions, leading to the mixing of saline strata with less saline strata, which is interpreted in this study as freshwater input. However, additional research is needed to confirm this possibility.

Lastly, the low organic interval is characterized by low TOC (<5%) accompanied by significant changes in parameters such as increased detrital input (Al%), reduction in redox condition proxies, and primary productivity proxies (primarily Cu/Al). This change occurs abruptly in the shallower core (SC-15) and gradually in the distal core (HV-54), which may reflect differences in environmental evolution or simply sampling spacing. These samples in the plot of Figure 10 differ from others by their higher Cd/Mo values, indicating a non-restricted environment.

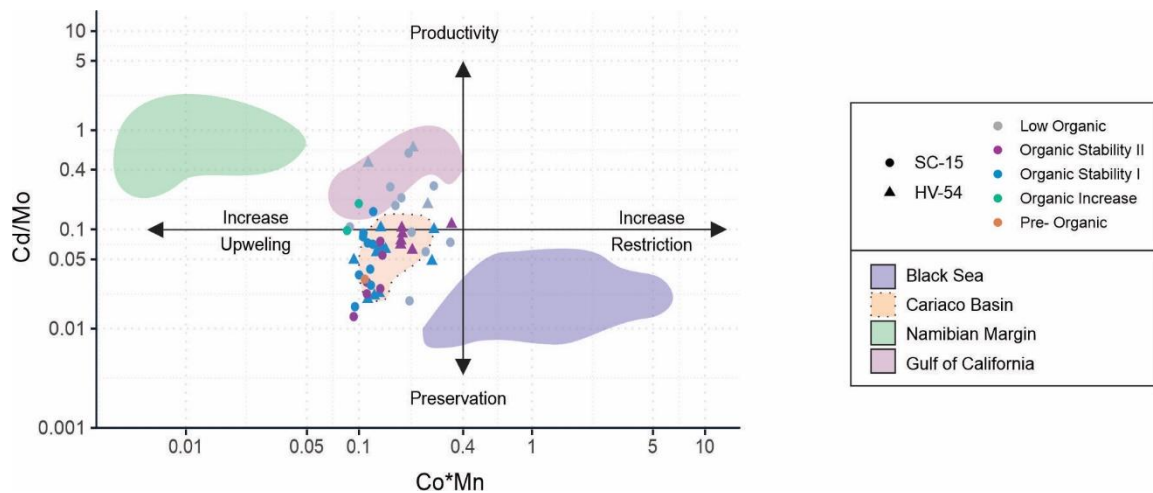


Fig. 10 – Plot of Cd/Mo v Co (mg/kg)\*Mn (%) environmental fields and data from Sweere et al. (2016).

## 6. Conclusions

The integration of stratigraphic, petrographic, and detailed geochemical

analyses of two wells in the Irati Formation in the southern Paraná Basin provided insights into the paleoenvironmental deposition of the Irati-Whitehill Sea. The development of anoxia in this restricted marine/lacustrine environment was elucidated through chemostratigraphy, which allowed for the subdivision of lithologically homogeneous intervals.

The pre-Organic interval reflects deposition in a saline environment, occurring under oxic conditions, with low detrital input and low primary productivity, registering less than 5% TOC. Subsequently, the Organic Increment interval indicates a transition to an environment that facilitated the accumulation and preservation of organic matter (OM). During this interval, TOC reaches close to 10%, accompanied by increased primary productivity and reduced salinity. During the Organic Stability interval, the highest concentration of organic matter occurs, with TOC reaching 10-15%, alongside a positive excursion in organic carbon isotopes. This interval is characterized by continued high primary productivity and low salinity. The correlation between these parameters may be related to increased primary productivity and reduced salinity, potentially due to a freshwater influx. The restricted environment of the target interval resembles the hybrid dynamics of the Cariaco Basin, which experiences episodic upwellings. The episodic influx of freshwater into the restricted Irati-Whitehill Sea system led to phytoplankton blooms, causing oxygen depletion to anoxic/euxinic conditions and facilitating the preservation of organic matter (OM). Although freshwater input is considered a key trigger for anoxia, the studies in this work were not conclusive regarding its source. This significant accumulation of organic matter is followed by a return to environmental conditions that result in low organic content (<5%). This is accompanied by substantial changes in parameters, including a return to an oxygenated environment with low primary productivity and an increase in detrital input.

### **Acknowledgements**

This study is part of the PETROBRAS project (00500071791119), whose financial support and partnership were essential for the execution of this work. It was also supported by the Human Resource Program of the Brazilian National Agency for Petroleum, Natural Gas, and Biofuels (PRH-ANP), with resources provided by oil companies under contract clause No. 50/2015 of R, D&I of the ANP.



## References

- Algeo, Thomas J., & Li, C. 2020. Redox classification and calibration of redox thresholds in sedimentary systems. *Geochimica et Cosmochimica Acta*, 287: 8–26.
- Algeo, Thomas J., & Lyons, T. W. 2006. Mo–total organic carbon covariation in modern anoxic marine environments: Implications for analysis of paleoredox and paleohydrographic conditions. *Paleoceanography*, 21(1): 2004PA001112.
- Algeo, Thomas J., & Maynard, J. B. 2008. Trace-metal covariation as a guide to water-mass conditions in ancient anoxic marine environments. *Geosphere*, 4(5): 872–887.
- Algeo, T.J., & Tribovillard, N. 2009. Environmental analysis of paleoceanographic systems based on molybdenum–uranium covariation. *Chemical Geology*, 268(3–4): 211–225.
- Antunes, G. C., Warren, L. V., Okubo, J., Fairchild, T. R., Varejão, F. G., Uhlein, G. J., Inglez, L., Poiré, D. G., Bahniuk, A. M., & Simões, M. G. 2022. The rise and fall of the giant stromatolites of the Lower Permian Irati Formation (Paraná Basin, Brazil): A multi-proxy based paleoenvironmental reconstruction. *Palaeogeography, Palaeoclimatology, Palaeoecology*, 606: 111246.
- Araújo, L. 2001a. Análise da expressão estratigráfica dos parâmetros de geoquímica orgânica e inorgânica nas sequencias Irati. *Porto Alegre. 2v., 301p. Tese de Doutorado em Geociências, Instituto de Geociências, Universidade Federal do Rio Grande do Sul.*
- Araújo, L. 2001b. Análise da expressão estratigráfica dos parâmetros de geoquímica orgânica e inorgânica nas sequências deposicionais Irati. *Unpublished PhD thesis*, 2: .
- Arthur, M., & Sageman, B. 1994. Marine black shales: A review of depositional mechanisms and environments of ancient deposits: *Annual Review Earth and Planetary Sciences*, v. 22. *Cité en*, 26.
- Bastos, L. P. H., Rodrigues, R., Pereira, E., Bergamaschi, S., Alferes, C. L. F., Augland, L. E., Domeier, M., Planke, S., & Svensen, H. H. 2021. The birth and demise of the vast epicontinental

- Permian Irati-Whitehill sea: Evidence from organic geochemistry, geochronology, and paleogeography. *Palaeogeography, Palaeoclimatology, Palaeoecology*, 562: 110103.
- Berner, R. A., & Raiswell, R. 1984. C/S method for distinguishing freshwater from marine sedimentary rocks. *Geology*, 12(6): 365–368.
- Bond, D., Wignall, P. B., & Racki, G. 2004. Extent and duration of marine anoxia during the Frasnian–Famennian (Late Devonian) mass extinction in Poland, Germany, Austria and France. *Geological Magazine*, 141(2): 173–193.
- Brito, A. S., Nogueira, A. C. R., Dos Santos, R. F., Angélica, R. S., & Rodrigues, R. 2024. High-frequency palaeoenvironmental changes in the mixed siliciclastic–carbonate sedimentary system from a lower Permian restricted basin (West Gondwana, southern Brazil). *Sedimentology*, 71(5): 1515–1557.
- Bruland, K. W. 1980. Oceanographic distributions of cadmium, zinc, nickel, and copper in the North Pacific. *Earth and Planetary Science Letters*, 47(2): 176–198.
- Brumsack, H. J. 1986. The inorganic geochemistry of Cretaceous black shales (DSDP Leg 41) in comparison to modern upwelling sediments from the Gulf of California. *Geological Society, London, Special Publications*, 21(1): 447–462.
- Burchette, T. P., & Wright, V. P. 1992. Carbonate ramp depositional systems. *Sedimentary geology*, 79(1–4): 3–57.
- Cagliari, J., Serratt, H., Cassel, M. C., Schmitz, M. D., & Chemale Jr., F. 2022. New high-precision U-Pb zircon age of the Irati Formation (Paraná Basin) and implications for the timing of the Kungurian anoxic events recorded in southern Gondwana. *Gondwana Research*, 107: 134–145.
- Capone, D. G., & Kiene, R. P. 1988. Comparison of microbial dynamics in marine and freshwater sediments: Contrasts in anaerobic carbon catabolism 1. *Limnology and oceanography*, 33(4part2): 725–749.
- Carmichael, S. K., Waters, J. A., Suttner, T. J., Kido, E., & DeReuil, A. A. 2014. A new model for the Kellwasser Anoxia Events (Late Devonian): Shallow water anoxia in an open oceanic setting

in the Central Asian Orogenic Belt. *Palaeogeography, Palaeoclimatology, Palaeoecology*, 399: 394–403.

da S. Ramos, A., Rodrigues, L. F., de Araujo, G. E., Pozocco, C. T. M., Ketzer, J. M. M., Heemann, R., & Lourega, R. V. 2015. Geochemical Characterization of Irati And Palermo Formations (Paraná Basin–Southern Brazil) for Shale Oil/Gas Exploration. *Energy Technology*, 3(5): 481–487.

Demaison, G. J., & Moore, G. T. 1980. Anoxic environments and oil source bed genesis. *Organic Geochemistry*, 2(1): 9–31.

Goddéris, Y., & Joachimski, M. M. 2004. Global change in the Late Devonian: modelling the Frasnian–Famennian short-term carbon isotope excursions. *Palaeogeography, Palaeoclimatology, Palaeoecology*, 202(3–4): 309–329.

Goldberg, K., & Goldberg Da Rosa, L. 2024. Applying Statistical Analysis and Economics Models to Unscramble the Depositional Signals from Chemical Proxies in Black Shales. *Geosciences*, 14(2): 43.

Goldberg, K., & Humayun, M. 2016. Geochemical paleoredox indicators in organic-rich shales of the Irati Formation, Permian of the Paraná Basin, southern Brazil. *Brazilian Journal of Geology*, 46(3): 377–393.

Guan, M., Wu, S., Hou, L., Jiang, X., Ba, D., & Hua, G. 2021. Paleoenvironment and chemostratigraphy heterogeneity of the Cretaceous organic-rich shales. *Advances in Geo-Energy Research*, 5(4): 444–455.

Hachiro, J. 1997. *O Subgrupo Irati (Neopermiano) da Bacia do Paraná*. text, Universidade de São Paulo.

Hatch, J. R., & Leventhal, J. S. 1992. Relationship between inferred redox potential of the depositional environment and geochemistry of the Upper Pennsylvanian (Missourian) Stark Shale Member of the Dennis Limestone, Wabaunsee County, Kansas, U.S.A. *Chemical Geology*, 99(1): 65–82.

- Holz, M., França, A. B., Souza, P. A., Iannuzzi, R., & Rohn, R. 2010. A stratigraphic chart of the Late Carboniferous/Permian succession of the eastern border of the Paraná Basin, Brazil, South America. *Journal of South American Earth Sciences*, 29(2): 381–399.
- Jenkyns, H. C. 2010. Geochemistry of oceanic anoxic events: REVIEW. *Geochemistry, Geophysics, Geosystems*, 11(3): n/a-n/a.
- Jones, B., & Manning, D. A. C. 1994. Comparison of geochemical indices used for the interpretation of palaeoredox conditions in ancient mudstones. *Chemical Geology*, 111(1): 111–129.
- LaGrange, M. T., Konhauser, K. O., Catuneanu, O., Harris, B. S., Playter, T. L., & Gingras, M. K. 2020. Sequence stratigraphy in organic-rich marine mudstone successions using chemostratigraphic datasets. *Earth-Science Reviews*, 203: 103137.
- Lyons, T. W., & Severmann, S. 2006. A critical look at iron paleoredox proxies: New insights from modern euxinic marine basins. *Geochimica et Cosmochimica Acta*, 70(23): 5698–5722.
- Lyons, T. W., Werne, J. P., Hollander, D. J., & Murray, R. W. 2003. Contrasting sulfur geochemistry and Fe/Al and Mo/Al ratios across the last oxic-to-anoxic transition in the Cariaco Basin, Venezuela. *Chemical Geology*, 195(1–4): 131–157.
- Martins, Laercio L., Schulz, H.-M., Noah, M., Poetz, S., Severiano Ribeiro, H. J. P., & da Cruz, G. F. 2021. New paleoenvironmental proxies for the Irati black shales (Paraná Basin, Brazil) based on acidic NSO compounds revealed by ultra-high resolution mass spectrometry. *Organic Geochemistry*, 151: 104152.
- Martins, Laercio Lopes, Schulz, H.-M., Severiano Ribeiro, H. J. P., Nascimento, C. A. do, Souza, E. S. de, & da Cruz, G. F. 2020. Organic geochemical signals of freshwater dynamics controlling salinity stratification in organic-rich shales in the Lower Permian Irati Formation (Paraná Basin, Brazil). *Organic Geochemistry*, 140: 103958.
- McArthur, J., Algeo, T., Van de Schootbrugge, B., Li, Q., & Howarth, R. 2008. Basinal restriction, black shales, Re-Os dating, and the Early Toarcian (Jurassic) oceanic anoxic event. *Paleoceanography*, 23(4): .

- McArthur, J. M. 2019. Early Toarcian black shales: A response to an oceanic anoxic event or anoxia in marginal basins? *Chemical Geology*, 522: 71–83.
- Milani, E., França, A., & Medeiros, R. 2007. Roteiros Geológicos, Rochas geradoras e rochas reservatório da Bacia do Paraná. *Boletim de Geociências da Petrobras*, 15(1): 135–162.
- Milani, Edison J., & Ramos, V. A. 1998. OROGENIAS PALEOZÓICAS NO DOMÍNIO SUL-OCCIDENTAL DO GONDWANA E OS CICLOS DE SUBSIDÊNCIA DA BACIA DO PARANÁ. *Revista Brasileira de Geociências*, 28(4): 473–484.
- Milani, Edison José, Rangel, H. D., Bueno, G. V., Stica, J. M., Winter, W. R., Caixeta, J. M., Neto, O. P., & others. 2007. Bacias sedimentares brasileiras: cartas estratigráficas. *Boletim de Geociências da PETROBRAS*, 15(2): 183–205.
- Murphy, A. E., Sageman, B. B., Hollander, D. J., Lyons, T. W., & Brett, C. E. 2000. Black shale deposition and faunal overturn in the Devonian Appalachian Basin: Clastic starvation, seasonal water-column mixing, and efficient biolimiting nutrient recycling. *Paleoceanography*, 15(3): 280–291.
- Nascimento, C. A. do, Souza, E. S. de, Martins, L. L., Severiano Ribeiro, H. J. P., Santos, V. H., & Rodrigues, R. 2021. Changes in depositional paleoenvironment of black shales in the Permian Irati Formation (Paraná Basin, Brazil): Geochemical evidence and aromatic biomarkers. *Marine and Petroleum Geology*, 126: 104917.
- Oehlert, A. M., & Swart, P. K. 2014. Interpreting carbonate and organic carbon isotope covariance in the sedimentary record. *Nature Communications*, 5(1): 4672.
- OELOFSEN, B., & ARAUJO, D. C. 1983. Palaecological implications of the distribution of mesosaurid reptiles in the Permian Irati sea (Paraná Basin), South America. *Revista Brasileira de Geociências*, 13(1): 1–6.
- Oelofsen, B. W. 1981. *An anatomical and systematic study of the family Mesosauridae (Reptilia: Proganosauria) with special reference to its associated fauna and palaeoecological environment in the Whitehill Sea*. PhD Thesis, Stellenbosch: Stellenbosch University.

- Percival, L. M. E., Bond, D. P. G., Rakociński, M., Marynowski, L., Hood, A. v. S., Adatte, T., Spangenberg, J. E., & Föllmi, K. B. 2020. Phosphorus-cycle disturbances during the Late Devonian anoxic events. *Global and Planetary Change*, 184: 103070.
- Petri, S., Fonseca Giannini, P. C., Chahud, A., & Sayeg, I. J. 2022. Tepees associated with mobility of evaporite sulfate: The case of the Irati Formation, Permian of Paraná Basin, Brazil. *Journal of Sedimentary Research*, 92(11): 1053–1070.
- Pujol, F., Berner, Z., & Stüben, D. 2006. Palaeoenvironmental changes at the Frasnian/Famennian boundary in key European sections: Chemostratigraphic constraints. *Palaeogeography, Palaeoclimatology, Palaeoecology*, 240(1–2): 120–145.
- Rau, G. H., Takahashi, T., Des Marais, D. J., Repeta, D. J., & Martin, J. H. 1992. The relationship between  $\delta^{13}\text{C}$  of organic matter and  $[\text{CO}_2(\text{aq})]$  in ocean surface water: Data from a JGOFS site in the northeast Atlantic Ocean and a model. *Geochimica et Cosmochimica Acta*, 56(3): 1413–1419.
- Rocha-Campos, A. C., Basei, M. A. S., Nutman, A. P., Santos, P. R., Passarelli, C. R., Canile, F. M., Rosa, O. C. R., Fernandes, M. T., Santa Ana, H., & Veroslavsky, G. 2019. U-Pb Zircon Dating of Ash Fall Deposits from the Paleozoic Paraná Basin of Brazil and Uruguay: A Reevaluation of the Stratigraphic Correlations. *The Journal of Geology*, 127(2): 167–182.
- Sageman, B. B., & Lyons, T. W. 2003. Geochemistry of Fine-grained Sediments and Sedimentary Rocks. *In: Treatise on Geochemistry*. Elsevier, p.115–158.
- Santos, R. V., Souza, P. A., De Alvarenga, C. J. S., Dantas, E. L., Pimentel, M. M., De Oliveira, C. G., & De Araújo, L. M. 2006. Shrimp U–Pb zircon dating and palynology of bentonitic layers from the Permian Irati Formation, Paraná Basin, Brazil. *Gondwana Research*, 9(4): 456–463.
- Schmitz, B., Charisi, S. D., Thompson, E. I., & Speijer, R. P. 1997. Barium,  $\text{SiO}_2$  (excess), and  $\text{P}_2\text{O}_5$  as proxies of biological productivity in the Middle East during the Palaeocene and the latest Palaeocene benthic extinction event. *Terra Nova*, 9(2): 95–99.

- Schneider, R., Mühlmann, H., Tommasi, E., Medeiros, R. de, Daemon, R. F., Nogueira, A., & others. 1974. Revisão estratigráfica da Bacia do Paraná. *Congresso brasileiro de Geologia*, p.41–65.
- Segarra, K. E. A., Comerford, C., Slaughter, J., & Joye, S. B. 2013. Impact of electron acceptor availability on the anaerobic oxidation of methane in coastal freshwater and brackish wetland sediments. *Geochimica et Cosmochimica Acta*, 115: 15–30.
- Shu, Y., Lu, Y., Hu, Q., Wang, C., & Wang, Q. 2021. Geochemical, petrographic and reservoir characteristics of the transgressive systems tract of lower Silurian black shale in Jiaoshiba area, southwest China. *Marine and Petroleum Geology*, 129: 105014.
- Sim, M. S., Ono, S., & Hurtgen, M. T. 2015. Sulfur isotope evidence for low and fluctuating sulfate levels in the Late Devonian ocean and the potential link with the mass extinction event. *Earth and Planetary Science Letters*, 419: 52–62.
- Souza, P. A. 2006. Late carboniferous palynostratigraphy of the Itararé subgroup, northeastern Paraná Basin, Brazil. *Review of Palaeobotany and Palynology*, 138(1): 9–29.
- Souza, P. A., Félix, C. M., Premaor, E., Boardman, D. R., Beri, Á., & Bender, R. R. 2023. Ice-Hothouse Transition and Palynological Evidences in Brazil. *In: Brazilian Paleofloras: From Paleozoic to Holocene*. Springer, p.1–32.
- Souza, P. A., & Marques-Toigo, M. 2005. Progress on the palynostratigraphy of the Permian strata in Rio Grande do Sul State, Paraná Basin, Brazil. *Anais da Academia Brasileira de Ciências*, 77(2): 353–365.
- Sunda, W. 2012. Feedback Interactions between Trace Metal Nutrients and Phytoplankton in the Ocean. *Frontiers in Microbiology*, 3: .
- Sweere, T., van den Boorn, S., Dickson, A. J., & Reichart, G.-J. 2016. Definition of new trace-metal proxies for the controls on organic matter enrichment in marine sediments based on Mn, Co, Mo and Cd concentrations. *Chemical Geology*, 441: 235–245.
- Tribovillard, N. 2021. Re-assessing copper and nickel enrichments as paleo-productivity proxies. *Bulletin de la Société Géologique de France*, 192(1): 54.

- Tyson, R., & Pearson, T. 1991. Modern and ancient continental shelf anoxia: An overview. *Geological Society, London, Special Publications*, 58: 1–24.
- Wang, Q., Huang, Y., Zhang, Z., Wang, C., & Li, X. 2022. Application of Chemical Sequence Stratigraphy to the Prediction of Shale Gas Sweet Spots in the Wufeng and Lower Longmaxi Formations within the Upper Yangtze Region. *Minerals*, 12(7): 859.
- Wedepohl, K. H. 1971. Environmental influences on the chemical composition of shales and clays. *Physics and Chemistry of the Earth*, 8: 307–333.
- Wei, W., & Algeo, T. J. 2020. Elemental proxies for paleosalinity analysis of ancient shales and mudrocks. *Geochimica et Cosmochimica Acta*, 287: 341–366.
- Xavier, P. L. A., Silva, A. F., Soares, M. B., Horn, B. L. D., & Schultz, C. L. 2018. Sequence stratigraphy control on fossil occurrence and concentration in the epeiric mixed carbonate-siliciclastic ramp of the Early Permian Irati Formation of southern Brazil. *Journal of South American Earth Sciences*, 88: 157–178.
- Zhai, G., Li, J., Jiao, Y., Wang, Y., Liu, G., Xu, Q., Wang, C., Chen, R., & Guo, X. 2019. Applications of chemostratigraphy in a characterization of shale gas Sedimentary Microfacies and predictions of sweet spots —taking the Cambrian black shales in Western Hubei as an example. *Marine and Petroleum Geology*, 109: 547–560.
- Zhang, C., Fang, C., Zhao, Q., Meng, G., Zhou, D., Li, J., & Shao, W. 2023. Multi-Proxies Analysis of Organic Matter Accumulation of the Late Ordovician–Early Silurian Black Shale in the Lower Yangtze Region, South China. *Minerals*, 13(3): 400.
- Zhao, J., Jin, Z., Jin, Z., Geng, Y., Wen, X., & Yan, C. 2016. Applying sedimentary geochemical proxies for paleoenvironment interpretation of organic-rich shale deposition in the Sichuan Basin, China. *International Journal of Coal Geology*, 163: 52–71.



## ANEXO A – COMPROVANTES DE SUBMISSÃO DO ARTIGO

---

### Confirming submission to Palaeogeography, Palaeoclimatology, Palaeoecology

2 messages

---

**Palaeogeography, Palaeoclimatology, Palaeoecology** <em@editorialmanager.com>

Thu, Aug 29, 2024 at 2:15  
PM

Reply-To: "Palaeogeography, Palaeoclimatology, Palaeoecology" <support@elsevier.com>

To: Jhenifer Silva Paim <jheniferpaimufrgs@gmail.com>

\*This is an automated message.\*

Geochemical Insights into Paleoenvironmental Influences on Organic-Rich Shale Deposition in the Irati-Whitehill Sea, Southern Paraná Basin

Dear Ms. Silva Paim,

We have received the above referenced manuscript you submitted to Palaeogeography, Palaeoclimatology, Palaeoecology.

To track the status of your manuscript, please log in as an author at <https://www.editorialmanager.com/palaeo/>, and navigate to the "Submissions Being Processed" folder.

Thank you for submitting your work to this journal.

Kind regards,  
Palaeogeography, Palaeoclimatology, Palaeoecology

1.2

ANEXO I	
Título da Dissertação:	
<b>"INSIGHTS GEOQUÍMICOS SOBRE AS INFLUÊNCIAS PALEOAMBIENTAIS NA DEPOSIÇÃO DE FOLHELHOS RICOS EM MATÉRIA ORGÂNICA NO MAR IRATI-WHITEHILL, SUL DA BACIA DO PARANÁ"</b>	
Área de Concentração: Estratigrafia	
Autora: <b>Jhenifer Caroline da Silva Paim</b>	
Orientadora: Profa. Dra. Juliana Charão Marques (PPGGEO/UFRGS) Coorientadora: Profa. Dra. Karin Goldberg (Kansas State University)	
Examinadora: Profa. Dra. Tais Freitas da Silva	
Data: 10/09/2024	
Conceito: A	
<p style="text-align: center;"><b>PARECER:</b></p> <p>A dissertação apresentada cumpre os requisitos exigidos pelo PPGGEO com apresentação do texto integrador, artigo submetido e carta de submissão para revista de qualis Capes A. O tema do trabalho é bastante importante com grande contribuição para as discussões sobre deposição e preservação da matéria orgânica em folhelhos. O texto está bem apresentação com poucos erros ortográficos. Porém, sugere-se revisão das citações e referências bibliográficas. Em relação ao artigo submetido, os revisores da revista farão os comentários, mas quero mencionar que os resultados obtidos são apresentados de forma concisa e muito bem trabalhados ao longo do texto. As discussões, interpretações e conclusões são coerentes, e consistentes com dados da literatura. Portanto, o referido trabalho de mestrado apresenta elevada qualidade técnico-científica e acadêmica, se constituindo em documento de importante contribuição para a Geologia.</p>	
Assinatura:	<p>TAIS FREITAS DA SILVA:94471967 053</p> <p><small>Assinado de forma digital por TAIS FREITAS DA SILVA:94471967053 Dados: 2024.09.09 15:02:30 -03'00'</small></p>
Ciente do Orientador:	
Ciente do Aluno:	

<b>ANEXO I</b>	
Título da Dissertação:	
<b>“INSIGHTS GEOQUÍMICOS SOBRE AS INFLUÊNCIAS PALEOAMBIENTAIS NA DEPOSIÇÃO DE FOLHELHOS RICOS EM MATÉRIA ORGÂNICA NO MAR IRATI-WHITEHILL, SUL DA BACIA DO PARANÁ”</b>	
Área de Concentração: Estratigrafia	
Autora: <b>Jhenifer Caroline da Silva Paim</b>	
Orientadora: Profa. Dra. Juliana Charão Marques (PPGGEO/UFRGS) Coorientadora: Profa. Dra. Karin Goldberg (Kansas State University)	
Examinador: Prof. Dr. Ailton da Silva Brito	
Data: 10/09/2024	
Conceito: A	
<b>PARECER:</b>	
A discente fez uma excelente apresentação, com uma variedade de dados em sedimentologia e geoquímica. A seguir alguns pontos que necessitam de revisão: (i) A descrição e apresentação dos dados sedimentológicos necessitam de revisão, desde a tabela da fácies a descrição e apresentação das associações de fácies devido haver a ausência de associação/fácies diagnósticas em uma das três associações; (ii) Há a necessidade de correlação e discussão dos os dados com queles já presentes na literatura sobre os intervalos orgânicos apresentados pela discente, pois já existem esse tipo de estruturação para a Formação na literatura.	
Assinatura:	Data: 10/09/2024
Ciente do Orientador:	
Ciente do Aluno:	

ANEXO I	
Título da Dissertação:	
<b>“INSIGHTS GEOQUÍMICOS SOBRE AS INFLUÊNCIAS PALEOAMBIENTAIS NA DEPOSIÇÃO DE FOLHELHOS RICOS EM MATÉRIA ORGÂNICA NO MAR IRATI-WHITEHILL, SUL DA BACIA DO PARANÁ”</b>	
Área de Concentração: Estratigrafia	
Autora: <b>Jhenifer Caroline da Silva Paim</b>	
Orientadora: Profa. Dra. Juliana Charão Marques (PPGGEO/UFRGS) Coorientadora: Profa. Dra. Karin Goldberg (Kansas State University)	
Examinadora: Dra. Rosalia Barili Da Cunha	
Data: 10/09/2024	
Conceito: B	
PARECER:	
<p>Jhenifer defendeu muito bem a dissertação, evidenciando na apresentação alguns pontos que não foram indicados no texto da dissertação. Demonstra domínio em relação a aplicação da análise estratigráfica bem como dos <i>proxies</i> aplicados para um melhor entendimento da situação paleoambiental que preservou a matéria orgânica no intervalo, capacidade de integração de dados e informações e capacidade para discussão. Entretanto, é necessário pontuar alguns problemas relacionados a falta de revisão, os quais pontuo a seguir:</p>	
<ul style="list-style-type: none"><li>• A norma do PPGGEO indica a necessidade de um texto explicativo da estrutura da dissertação, o qual não foi inserido.</li><li>• Não apresenta listas de figuras, quadro e tabelas.</li><li>• Não aponta, na estrutura da dissertação, alguns dos itens pontuados pela norma. Apesar de presentes, é necessário seguir a estrutura indicada pela norma.</li><li>• Falta de padronização das citações de referências.</li><li>• Falta de padronização nas citações de figuras.</li><li>• Os agradecimentos iniciam com uma frase padrão de IA indicando que houve uso desta ferramenta para melhoramento do texto, mas que não</li></ul>	

houve revisão criteriosa do documento. Não há problemas em melhorar o texto usando ferramentas de IA (principalmente partes que não têm relação direta com a geração de conteúdo inédito), mas é necessário que o texto passe por revisão.

- Outra evidência de falta de revisão é a parte em português no meio do abstract, que se repete no abstract do artigo.
- Partes do texto da dissertação parecem uma tradução do artigo. Não se espera que a dissertação, o texto integrador, seja apenas a tradução do artigo. Este é o espaço onde o candidato deve acrescentar todo o material complementar e revisão que não cabe no artigo por motivos de escopo do periódico e por ser realmente a parte onde evidencia-se que o trabalho empregado na pesquisa foi muito além de um artigo, envolvendo muito tempo para revisão conceitual, análise e integração de dados.
- Na síntese dos resultados e interpretações apresenta apenas as interpretações, e não os resultados.

Em relação ao conteúdo da dissertação, como já mencionado, é necessário pontuar que foram citados dados que não foram apresentados ou que mereciam uma maior atenção na discussão e que poderão tornar o artigo mais robusto quando retornar para revisão:

- A pesquisadora pontua que foram realizadas análises de DRX, inclusive citados na metodologia do artigo. Estes resultados não foram apresentados ou discutidos. São dados interessantes uma vez que a petrografia não foi realizada nas porções mais finas, e estes podem auxiliar na interpretação paleoambiental dado a identificação de argilominerais que elucidam processos deposicionais e diagenéticos específicos.
- No caso de um projeto maior, caso os dados não possam ser apresentados, mas foram usados, deve-se pontuar isto. Bem como dados que eventualmente foram gerados pelo projeto e não diretamente pelo estudante.
- Um ponto que deixa dúvida se foi falta de revisão, é quando menciona que foram descritos 70 metros da Formação Irati. São 70m de testemunho, não

um intervalo de tal espessura, composto por 32m em um poço e 38m no outro.

- Outro ponto de atenção é que no resumo menciona teores elevados de MO como 15% para o folhelho e no texto sobre litologia indica que pode chegar a 25% no folhelho inferior e o superior a 15%.
- Menciona o gráfico ternário de Si, Al e Ca, mas não apresenta o mesmo.
- As análises de isótopos de carbono orgânico foram citadas, apresentadas nos logs, evidenciando a excursão positiva no intervalo relacionado a deposição e preservação da MO. Entretanto, não é discutido o seu significado, o motivo de haver uma excursão positiva sendo que os teores de TOC do mesmo intervalo parecem relativamente estáveis, a extensão desta excursão na bacia, se ocorre apenas localmente, se é um evento regional ou global. Não há revisão sobre este assunto na dissertação, o que complementaria os demais proxies utilizados para um melhor entendimento do sistema, tornando a discussão ainda mais robusta.
- Não são apresentados os dados brutos de forma geral, a não ser nos logs. Os dados brutos, principalmente de FRX, devem ser apresentados como apêndices, caso não seja possível apresentá-los em forma de tabela no corpo da dissertação. Nos logs não é possível avaliar o controle de qualidade destes dados, por exemplo.
- Não apresenta a correlação de poços da região, que foi apresentada na defesa. Tal informação é útil para corroborar ou refutar as ideias apresentadas e embasar suas interpretações.

Assinatura:

Data: 13/09/2024

Ciente do Orientador:

Ciente do Aluno: